

UNIVERSIDADE DE LISBOA
FACULDADE DE CIÊNCIAS
DEPARTAMENTO DE QUÍMICA E BIOQUÍMICA



**DEVELOPMENT OF NEW APPROACHES FOR MICRO-
EXTRACTION: Application of microfluidic devices and
novel sorption-based polymers**

Marta Pacheco Botelho Mourão

DISSERTAÇÃO
MESTRADO EM QUÍMICA
QUÍMICA ANALÍTICA

2012

UNIVERSIDADE DE LISBOA
FACULDADE DE CIÊNCIAS
DEPARTAMENTO DE QUÍMICA E BIOQUÍMICA



**DEVELOPMENT OF NOVEL APPROACHES FOR
MICRO-EXTRACTION: Application of microfluidic devices
and novel sorption-based polymers**

Marta Pacheco Botelho Mourão

Thesis supervised by Professor Dr. José Manuel Florêncio Nogueira
(FCUL) and Professor Dr. Ir. Hans-Gerd Janssen (UvA)

MESTRADO EM QUÍMICA
QUÍMICA ANALÍTICA
2012

Acknowledgments

First to my advisor, Prof. Dr. José M. F. Nogueira, because without him it would be impossible to develop the project in question. Thank you for the opportunity to work in your research group and area, the availability, the support, the dedication, the transmission of knowledge, the absolute and positive encouragement and for making possible that half of my work was made in the University of Amsterdam.

To Prof. Dr. Ir. Peter Schoenmakers and Prof. Dr. Ir. Hans-Gerd Janssen for giving me the change to do a part of my thesis in their research group in the University of Amsterdam. Thank you for all of your criticism and advices. Also, thank you to the entire research group for your friendship, help and patience during my period there, especially to Daniela Peroni.

Thank you to all the friends I made in Amsterdam...you are amazing.

To my Portuguese lab mates in particular to Carlos Almeida, for the extreme availability, the friendliness, the suggestions and the patience to put up with me; to Nuno Neng for the tips provided and the exchange of ideas; to Bruno Boto and Rodrigo Bernarda for the friendship, the distracting times listening to music, the kind words said when something was not as it should be according to me, the company for having lunch and getting the liquid nitrogen.

A very special thank you to Catarina Carapeta, Andreia Alegre and João França for the dedicated support and encouragement, the constant company, the great friendship and the friendly words uttered.

To all of my long-time friends, particularly to Vânia Rodrigues for giving me the best summer week ever in Zambujeira do Mar (Portugal), for the great friendship, the advices given and the company.

To my lovely cousin, Ana Parreira for all the support, the company and for distracting me when I needed.

Last but not least, to my family, specifically my parents for all the unconditional love and support and for showing interest in understanding my work. I hope I can make them proud for many more years...

Thank you all!

Marta Mourão

Abstract

The present work includes two distinct parts aiming to develop and apply new micro-extraction approaches for trace analysis using microfluidic devices and novel sorption-based polymers. In the first part, microfluidic devices (“chips”) with different sizes and geometries were studied in dynamic mode, in which the performance was evaluated in terms of flow rate, sample volume, repeatability and efficiency using liquid desorption (LD). The devices were then applied in the extraction of fatty acid methyl esters, toluene, ethylbenzene, xylene and benzene and polycyclic aromatic hydrocarbons used as model compounds in aqueous solutions, followed by gas chromatography with flame ionization detection (GC-FID). The linear shape and packed PDMS particles [(10.4 ± 0.10) mg], presented suitable results showing good repeatability ($RSD \leq 15\%$) and efficiency (75-93 %). However, due to the difficulty of packing the PDMS particles, the application of the methodology in aqueous matrices, surface water samples in particular, was performed in a qualitative way in order to demonstrate that these microfluidic devices could be applied in real situations. These studies were carried-out by using comprehensive two-dimensional GC with FID (GC \times GC-FID).

In the second part, polyurethanes (PUs) having cylindrical geometry were applied as innovative devices for micro-extraction using the sorption and mechanical properties of these polymers. Therefore, a new approach using PUs soaked with suitable solvents was applied operating under the static floating sampling mode. Assays performed with PUs soaked with dichloromethane (DCM), followed by LD and large volume injection-gas chromatography-coupled to mass spectrometry, operating under the selected ion monitoring mode [LVI-GC-MS(SIM)], showed good performance using atrazine, terbuthylazine, alachlor and benzo(a)pyrene as model compounds in aqueous samples. Under optimized experimental conditions average recovery yields between 50 and 75 % were achieved. Good linearity ($r^2 > 0.99$; up to 50.0 $\mu\text{g/L}$) and limits of detection below 0.50 $\mu\text{g/L}$. The application of this methodology to real matrices, namely surface, ground, tap and seawater samples was performed using the standard addition method, demonstrating good analytical performance and absence of matrix effects. The proposed methodology [PU μ E(DCM)-LD/LVI-GC-MS(SIM)] presented as main advantages the use of small amounts of sample and solvent, reduced analytical time and easy handling, associated to a fast, simple and remarkable analytical performance.

Resumo

O presente trabalho inclui duas partes distintas, tendo como objetivos desenvolver e aplicar novas abordagens de micro-extração para análise vestigial usando dispositivos microfluídicos e polímeros inovadores baseados em sorção. Na primeira parte, estudaram-se, no modo dinâmico, dispositivos microfluídicos (“chips”) com diferentes tamanhos e geometrias, tendo o desempenho sido avaliado relativamente a taxas de fluxo, volume de amostra, repetibilidade e eficiência usando a dessorção líquida (LD). Os dispositivos foram posteriormente aplicados na extração de ácidos gordos metilados, tolueno, xileno, etilbenzeno e benzeno e hidrocarbonetos aromáticos policíclicos, utilizados como compostos modelo em soluções aquosas, seguido de cromatografia em fase gasosa com detecção por ionização de chama (GC-FID). A forma linear e empacotada com partículas de PDMS [(10.4 ± 0.10) mg], apresentou resultados adequados com boa repetibilidade (RSD ≤ 15 %) e eficiência (75-93 %). No entanto, devido à dificuldade de empacotamento das partículas de PDMS, a aplicação da metodologia a matrizes aquosas, em particular água superficial, foi efetuada em termos qualitativos com o intuito de demonstrar que os dispositivos microfluídicos poderiam ser aplicados em situações reais. Estes estudos foram levados a cabo recorrendo a GC bidimensional abrangente com FID (GC×GC-FID).

Na segunda parte, poliuretanos (PUs) com geometria cilíndrica foram aplicados como dispositivos inovadores para micro-extração utilizando as propriedades sortivas e mecânicas destes polímeros. Neste sentido, uma nova abordagem usando PUs impregnados em solventes orgânicos convenientes foi aplicada operando no modo de amostragem flutuante estática. Ensaio efetuados com PUs impregnados em diclorometano (DCM), seguido de LD e posterior análise por GC com injeção de grandes volumes acoplada a espectrometria de massa operando no modo de monitorização de iões selecionados [LVI-GC-MS(SIM)], demonstraram bom desempenho usando atrazina, terbutilazina, alacloro e benzo(a)pireno como compostos modelo em amostras de água. Sob condições experimentais otimizadas foram obtidas recuperações médias compreendidas entre 50 e 75 %, boa linearidade ($r^2 > 0.99$; até 50.0 µg/L) e limites de detecção abaixo de 0.50 µg/L.

A aplicação desta metodologia a matrizes reais, nomeadamente água superficial, subterrânea, torneira e mar, foi efetuada com recurso ao método de adição padrão, tendo demonstrado bom desempenho analítico e ausência de efeitos de matriz. A metodologia proposta [PU μ E(DCM)-LD/LVI-GC-MS(SIM)] apresentou como principais vantagens a utilização de pequenas quantidades de amostra e solventes, tempo analítico reduzido e fácil manipulação, associada a rapidez, simplicidade e notável desempenho analítico.

Keywords

- Microfluidic devices
- Sorptive extraction techniques
- Polyurethane foams (PU)
- Comprehensive two-dimensional gas chromatography (GC×GC)
- Environmental water matrices

Palavras-chave

- Dispositivos microfluídicos
- Técnicas de extração sortiva
- Espumas de poliuretano (PU)
- Cromatografia gasosa bidimensional abrangente (GC×GC)
- Matrizes de água ambiental

Abbreviations and Symbols

°C	Celsius
μ	Micro
μg/L	Microgram per litre
μL	Microlitre
%	Percentage
a	Slope
ACN	Acetonitrile
ALA	Alachlor
ATZ	Atrazine
b	Interception
BaP	Benzo(a)pyrene
BTEX	Benzene, toluene, ethylbenzene, xylene
°C/min	Celsius per minute
c ₀	Content
DCM	Dichloromethane
EtAc	Ethyl acetate

FAMES	Fatty acid methyl esters
GC	Gas chromatography
GC-FID	Gas chromatography with a flame ionization detector
GC-MS	Gas chromatography coupled to mass spectrometry
GC×GC	Comprehensive two-dimensional gas chromatography
HPLC	High performance liquid chromatography
LC	Liquid chromatography
LD	Liquid desorption
LOD	Limit of detection
LOQ	Limit of quantification
LVI	Large volume injection
Log $K_{o/w}$	Octanol-water partitioning coefficient
M	mol/L
MeOH	Methanol
mg	milligrams
min	minutes
mL	Millilitre
mL/min	Millilitre per minute

mm	Millimetre
% (w/v)	Weight/volume percentage
NaCl	Sodium chloride
n-C ₆	n – hexane
PAHs	Polycyclic aromatic hydrocarbons
PDMS	Polydimethylsiloxane
pK _a	Acid dissociation constant
PU	Polyurethane foam
rpm	Rotations per minute
RSD	Relative standard deviation
r ²	Correlation coefficient
SAM	Standard addition method
SIM	Selected ion monitoring
S/N	Signal-to-noise ratio
TBZ	Terbuthylazine
% (v/v)	Volume/volume percentage

Index

Acknowledgments	iii
Abstract	v
Resumo	vi
Keywords.....	viii
Palavras-chave	ix
Abbreviations and Symbols.....	x
Index.....	xiii
Index of figures.....	xvi
Index of tables	xxi

Chapter 1 – Introduction..... 1

1.1 Modern sample preparation.....	1
1.2 Static and dynamic sampling modes.....	1
1.3 Sorption-based techniques.....	2
1.3.1 Solid-phase extraction (SPE)	3
1.3.2 Open-tubular trapping (OTT)	4
1.3.3 Stir bar sorptive extraction (SBSE).....	5
1.3.4 Bar adsorptive micro-extraction (BA μ E)	7
1.4 Analytical techniques.....	8
1.4.1 Gas chromatography (GC).....	8
1.4.2 Gas chromatography-mass spectrometry (GC-MS).....	12
1.4.3 Comprehensive two-dimensional gas chromatography (GC \times GC)	13
1.5 Aim	15

Chapter 2 – Experimental..... 16

2.1 Microfluidic devices	16
2.1.1 Chemicals and samples	16
2.1.2 Materials and equipment	16
2.1.3 Experimental Procedure	17
2.1.3.1 Preparation of the standard solutions	17
2.1.3.2 GC-FID and GC \times GC-FID conditions	18
2.1.3.3 Instrumental calibration.....	18

2.1.3.4	Preparation of the microfluidic devices.....	18
2.1.3.5	Performance evaluation.....	21
2.1.3.6	Application to environmental water matrices (GC×GC).....	22
2.2	Polyurethane foams	22
2.2.1	Chemicals and samples.....	22
2.2.2	Materials and equipment	23
2.2.3	Experimental procedure.....	24
2.2.3.1	Preparation of the standard solutions.....	24
2.2.3.2	GC-MS conditions	24
2.2.3.3	Preparation of the PU phases	25
2.2.3.4	Recovery assays and method validation.....	25
2.2.3.5	Application to environmental water matrices	27
Chapter 3	– Results and Discussion.....	28
3.1	Microfluidic devices.....	28
3.1.1	Instrumental conditions	28
3.1.2	Performance evaluation.....	29
3.1.2.1	First Chip	29
3.1.2.2	LC trap.....	30
3.1.2.2.1	Flow rates of sample	33
3.1.2.2.2	Repeatability	34
3.1.2.2.3	Flow rates of EtAc	36
3.1.2.2.4	Desorption efficiency	36
3.1.2.2.5	Sample volume.....	37
3.1.2.3	Round chip.....	39
3.1.2.4	Cylindrical chip.....	40
3.1.3	Application to environmental water matrices	44
3.2	Polyurethane foams	49
3.1.1	Instrumental conditions	49
3.1.2	Optimization of the PU μ E(DCM)-LD/LVI-GC-MS(SIM) methodology	51
3.1.2.1	Optimization of the LD	51
3.1.2.1.1	Effect of evaporation.....	51
3.1.2.1.2	Effect of the soaking and desorption solvent.....	52

3.1.2.1.3	Effect of LD parameters (number of steps)	54
3.1.2.2	Optimization of PU μ E	55
3.1.2.2.1	Effect of the agitation speed	55
3.1.2.2.2	Effect of the extraction time	56
3.1.2.2.3	Effect of the pH.....	57
3.1.2.2.4	Effect of an organic modifier	58
3.1.2.2.5	Effect of the ionic strength	59
3.1.3	Validation of PU μ E(DCM)-LD/LVI-GC-MS(SIM) methodology.....	60
3.1.4	Application to environmental water matrices	64
Chapter 4 – Conclusions and Future Work		65
Chapter 5 – Bibliography		67
Appendixes		74
Appendix I		74
I.1	Chromatogram.....	74
Appendix II.....		75
II.1	Linearity plots	75
II.2	Calibration plots	75
II.3	Regression plots	76
Appendix III		78
III.1	Speciation of the analytes as a function of the pH, obtained by the SPARCS program.....	78
Appendix IV.....		82
IV.1	Formulas.....	82
Appendix V		83
V.1	MSDS files of the solvents	83
V.2	MSDS files of the reagents	85
V.3	List of R-phrases	87
V.4	List of S-phrases.....	89

Index of figures

1. Introduction

Figure 1 – Schematic representation exemplifying an SPE cartridge.....	3
Figure 2 – Schematic representation exemplifying an OTT device.....	4
Figure 3 – Schematic representation exemplifying a SBSE device.....	5
Figure 4 – Reaction scheme of the formation of PU foams.....	6
Figure 5 – Schematic representation exemplifying the BA μ E device operating in the floating sampling mode.....	8
Figure 6 – Schematic representation of a typical GC system.....	9
Figure 7 – Schematic representation of FID.....	11
Figure 8 – Schematic representation of a typical GC-MS system.....	12
Figure 9 – Typical set-up of a GC \times GC system.....	14

2. Experimental

Figure 10 – Gas chromatograph equipped with a flame ionization detector used for GC-FID and GC \times GC-FID analysis.....	17
Figure 11 – First chip (5 cm \times 2 cm \times 0.5 cm).....	19
Figure 12 – Chip installed in a chip-holder.....	19
Figure 13 – Final experimental set up of the chip.....	19
Figure 14 – Materials for making the LC trap.	19
Figure 15 – The LC trap (5.5 cm of length).	20

Figure 16 – Round chip with two glued capillaries and PDMS particles inside.	20
Figure 17 – Cylindrical chip with two glued capillaries and PDMS particles inside. ...	20
Figure 18 – PDMS particles used for packing the microfluidic devices (size 0.80 mm).....	21
Figure 19 – GC-MS system used in the present work.....	23
Figure 20 – PU cylinders used in the present work.....	25
Figure 21 – Schematic representation of the PU operating in the floating sampling mode.....	26
Figure 22 – Conventional plastic syringe (5 mL) used in the back-extraction step.....	26

2.1 Results and Discussion

Figure 23 – Chromatogram of the first chip. Test sample 1 flushed at a flow rate of 0.50 mL/min with a plastic syringe.....	30
Figure 24 – Final experimental set up of the LC column.....	31
Figure 25 – New metal connection made to the nitrogen tube for the drying process.	32
Figure 26 – Chromatogram of the LC trap. Test sample 2 flushed at a flow rate of 0.50 mL/min and back flushes on the drying steps. 1 – FA ₆ , 2 – FA ₈ , 3 – FA ₁₀ , 4 – FA ₁₁ , 5 – FA ₁₂ , 6 – FA ₁₄	33
Figure 27 – The influence of different flow rates of sample (with 0.10 mL/min of flow of EtAc and 30 minutes of drying at 2 bar).....	33
Figure 28 – The influence of different flow rates of EtAc (with 0.50 mL/min of flow rate of sample and 30 minutes of drying at 1 bar).	36

Figure 29 – The influence of volume sample (with 0.20 mL/min of flow rate of sample, 0.10 mL/min of flow rate of EtAc and 30 minutes of drying at 1 bar).	38
Figure 30 – Drying system with a tip of a pipette inside the chip.	39
Figure 31 – Chromatogram of the standard (left) and the round chip(right) (with 0.50 mL/min of flow rate of sample, 0.10 mL/min of flow rate of EtAc and 2.5 bar of drying pressure). 1 – FA ₆ , 2 – FA ₈ , 3 – FA ₁₀ , 4 – FA ₁₁ , 5 – FA ₁₂ , 6 – FA ₁₄	40
Figure 32 – Chromatogram of the cylindrical chip: EtAc flushed (A) and EtAc back flushed (B) (at 0.50 mL/min of flow rate of sample, 0.10 mL/min of flow rate of EtAc and 2 bar of drying pressure). 1 – FA ₆ , 2 – FA ₈ , 3 – FA ₁₀ , 4 – FA ₁₁ , 5 – FA ₁₂ , 6 – FA ₁₄	41
Figure 33 – Chromatogram of the cylindrical chip [(9.1 ± 0.1) mg of PDMS particles], first (black) and second fraction (blue). Efficiencies of the second fraction are 32-34%. 1 – FA ₆ , 2 – FA ₈ , 3 – FA ₁₀ , 4 – FA ₁₁ , 5 – FA ₁₂ , 6 – FA ₁₄	41
Figure 34 – Chromatogram of the cylindrical chip [(14.1 ± 0.1) mg of PDMS particles], first (black) and second fraction (blue). Efficiencies of the second fraction are 21-23%. 1 – FA ₆ , 2 – FA ₈ , 3 – FA ₁₀ , 4 – FA ₁₁ , 5 – FA ₁₂ , 6 – FA ₁₄	42
Figure 35 – Chromatogram of the cylindrical chip [18.2 ± 0.1) mg of PDMS particles], first (black) and second fraction (blue). Efficiencies of the second fraction are 9-11%. 1 – FA ₆ , 2 – FA ₈ , 3 – FA ₁₀ , 4 – FA ₁₁ , 5 – FA ₁₂ , 6 – FA ₁₄	42
Figure 36 – Cylindrical chip with PDMS and glass beads inside.....	43
Figure 37 – 2D Chromatogram of the surface water sample, in split mode with a rate of 5 °C/min (top) and in splitless mode with a rate of 10 °C/min (bottom).....	45
Figure 38 – 2D Chromatogram of the surface water sample spiked with 0.050 µg/mL of BTEX and PAHs, in splitless mode, a flow rate of 2 mL/min and an acquisition delay of 300 seconds (top) and in split mode, a flow rate of 2 mL/min and an acquisition delay of 0 seconds (bottom).	46

Figure 39 – 2D Chromatogram of the clean water (top) and the surface water sample (bottom) spiked with 0.050 µg/mL of BTEX and PAHs, in split mode, with a flow rate of 2 mL/min and an acquisition delay of 0 seconds.	47
Figure 40 – 3D picture of the clean water (top) and the surface water sample (bottom) spiked with 0.050 µg/mL of BTEX and PAHs, in split mode, with a flow rate of 2 mL/min and an acquisition delay of 0 seconds.	48
Figure 41 – Effect of the evaporation step on the average recovery of ATZ, TBZ, ALA and B(a)P (extraction: 2 h at 1000 rpm) by PUµE(DCM)-LD/LVI-GC-MS(SIM).....	52
Figure 42 – Effect of the soaking (DCM) and desorption solvents on the average recovery of ATZ, TBZ, ALA and B(a)P (extraction: 2 h at 1000 rpm with the addition of some droplets of saturated NaCl solution) by PUµE(DCM)-LD/LVI-GC-MS (SIM).....	53
Figure 43 – Effect of the soaking (n-C6) and desorption solvents on the average recovery of ATZ, TBZ, ALA and B(a)P (extraction: 2 h at 1000 rpm with the addition of some droplets of saturated NaCl solution) by PUµE(n-C6)-LD/LVI-GC-MS (SIM).....	53
Figure 44 – Effect of the number of compressions and the addition of solvent (DCM) on the average back extraction efficiency of ATZ, TBZ, ALA and B(a)P (extraction: 2 h at 1000 rpm with the addition of some droplets of saturated NaCl solution) by PUµE(DCM)-LD/LVI-GC-MS(SIM).....	54
Figure 45 – Effect of the agitation speed on the average recovery of ATZ, TBZ, ALA and B(a)P (extraction: 2 h; 3 LD step with the addition of some droplets of saturated NaCl solution) by PUµE(DCM)-LD/LVI-GC-MS(SIM).....	55
Figure 46 – Effect of the extraction time on the average recovery of ATZ, TBZ, ALA and B(a)P (extraction: 1000 rpm; 3 LD step with the addition of some droplets of saturated NaCl solution) by PUµE(DCM)-LD/LVI-GC-MS(SIM).....	56
Figure 47 – Effect of the pH in the matrix on the average recovery of ATZ, TBZ, ALA and B(a)P (extraction: 30 min at 1000 rpm; 3 LD step with the addition of some droplets of saturated NaCl solution) by PUµE(DCM)-LD/LVI-GC-MS(SIM).....	57

Figure 48 – Effect of the addition of an organic modifier (MeOH) on the average recovery of ATZ, TBZ, ALA and B(a)P (extraction: 30 min at 1000 rpm, pH of 5.5; 3 LD step with the addition of some droplets of saturated NaCl solution) by PU μ E(DCM)-LD/LVI-GC-MS(SIM).....58

Figure 49 – Effect of the ionic strength (NaCl) on the average recovery of ATZ, TBZ, ALA and B(a)P (extraction: 30 min at 1000 rpm, pH of 5.5, 0 % of MeOH; 3 LD step with the addition of some droplets of saturated NaCl solution) by PU μ E(DCM)-LD/LVI-GC-MS(SIM).....60

Figure 50 – Calibration plots for the four compounds obtained by PU μ E(DCM)-LD/LVI-GC-MS(SIM) methodology, under optimized conditions.....63

Index of tables

3. Results and Discussion

Table 1 – Composition, octanol-water partitioning coefficients ($\log K_{o/w}$), retention times (RT) used to evaluate the performance of the different microfluidic devices.....	28
Table 2 – Within – day repeatability RSD values for each FAMES (at 0.20 mL/min of flow rate of sample, 0.10 mL/min of flow rate of EtAc and 2 bar of drying pressure).....	34
Table 3 – Within – day repeatability RSD values for each FAMES (at 0.20 mL/min of flow rate of sample, 0.10 mL/min of flow rate of EtAc and 1 bar of drying pressure).....	35
Table 4 – Between – day repeatability RSD values for each FAMES (at 0.20 mL/min of flow rate of sample, 0.10 mL/min of flow rate of EtAc and 1 bar of drying pressure).....	35
Table 5 – Desorption efficiencies (E) of the fraction for each FAMES at different flow rates of sample (with 0.10 mL/min of flow of EtAc and 30 minutes of drying at 2 bar).....	37
Table 6 – Optimize parameters with desorption efficiencies of the fractions between 74 and 93 % and RSD values lower than 15 %.....	38
Table 7 – Within – day repeatability RSD values for each FAMES (10 mL at 0.50 mL/min of flow rate of test sample 3, 0.020 mL/min of flow rate of EtAc back flushed and 2 bar of drying pressure, day one).....	43
Table 8 – Within – day repeatability RSD values for each FAMES (10 mL at 0.50 mL/min of flow rate of test sample 3, 0.020 mL/min of flow rate of EtAc back flushed and 2 bar of drying pressure, day two).....	44

Table 9 – Chemical formulas, octanol-water partitioning coefficients ($\log K_{o/w}$), retention times, pKa and ions selected for quantification in SIM mode of the compounds under study.....	49
Table 10 – LODs, LOQs, linear dynamic ranges, correlation coefficients (r^2) and precisions (RSD) obtained by GC-MS(SIM).....	50
Table 11 – Summary of the optimized conditions established for PU μ E(DCM)-LD/LVI-GC-MS(SIM) methodology.....	61
Table 12 – Average recoveries of the target compounds obtained under optimized conditions by PU μ E(DCM)-LD/LVI-GC-MS(SIM) methodology.....	61
Table 13 – Analytical limits (LOD and LOQ) for the compounds understudy obtained by PU μ E(DCM)-LD/LVI-GC-MS(SIM), under optimized conditions.....	62
Table 14 – Parameters of the method calibration [linear dynamic range, slope (a) and correlation coefficients (r^2)] obtained by PU μ E(DCM)-LD/LVI-GC-MS(SIM), under optimized conditions.....	62
Table 15 – Precision parameters, within – and between – day repeatability, RSD (%), obtained by PU μ E(DCM)-LD/LVI-GC-MS(SIM) methodology, under optimized conditions.....	63
Table 16 – Regression parameters obtained from SAM, under optimized conditions, for the water matrices studied using ATZ, TBZ, ALA and B(a)P as model compounds....	64

Chapter 1 – Introduction

1.1 Modern sample preparation

During the implementation of any analytical chemistry scheme several steps used to be included, such as extraction, concentration and many times derivatisation, prior to chromatographic or hyphenated techniques. So far, modern sample enrichment techniques are based on miniaturization, easy manipulation and absence of organic toxic solvents according to the principles of green analytical chemistry. For trace analysis of organic solutes in particular, the sorption-based methods have demonstrated to be a good choice for monitoring priority compounds. For example, solid phase extraction (SPE)^{1,2}, open-tubular trapping (OTT)³⁻⁵ and, more recently, the microfluidic devices (“chips”)⁶ are the most widely used dynamic sample preparation techniques. On the other hand, solid phase micro-extraction (SPME) and stir bar sorptive extraction (SBSE)^{1,2} are, nowadays, remarkable alternatives that operates under the static sampling mode.

1.2 Static and dynamic sampling modes

Most of the sample preparation techniques rely on the adsorption of the analytes of interest from the sample (liquid, solid or gas) by a porous material, followed by desorption and chromatographic analysis. However, only an aliquot (typically μL) of the extract is injected in the analytical instrument, resulting in a poor sensitivity of the method⁷. One possible solution includes the on-line combination of extraction with liquid chromatography and injection of large volumes in gas chromatography. The main principle of all sample preparation methods is the transfer of the compounds of interest from the sample matrix into a form more suitable for introduction into the analytical instrument⁷.

The first approach is called static sampling, which relies on the diffusion of the sample analytes into the extractant with the purpose of reaching equilibrium between both phases.

The selection of the extractant is based on the “like-like” principle, where a substance will always have more affinity for the phase with similar properties to those of the substance itself (nonpolar compounds should be extracted from a polar matrix by the use of a nonpolar extractant). The diffusion of the analytes can be promoted by certain procedures (stirring, shaking or sonification) that affect the time required for equilibration and not the equilibrium itself or other properties of the static process. The extraction efficiency is expressed as a percentage usually known as the recovery. SPME, SBSE and BaμE are good examples of this sampling mode^{3-6,8-10}.

On the other hand, in the dynamic sampling mode all the extractant is not immediately in contact with the sample. It is based on the use of a “stationary phase” (the extractant) and a moving mobile phase (the sample), resembling chromatographic techniques. In this case procedures such as stirring, shaking or sonification ensure complete extraction instead of promoting a faster equilibrium. Gaseous and liquid samples are usually pumped through the extractant that can be a packed bed²⁰, for instance, in which the breakthrough volume is a very important parameter since it determines the maximum volume of sample that can be flushed through the trapping device before the analytes are no longer sufficiently retained. SPE, OTT and, more recently, the microfluidic devices illustrate some good examples of dynamic sampling processes^{1,11-13,14-21}.

1.3 Sorption-based techniques

Over the years, the sorption-based techniques have proven to be powerful and environmental friendly approaches in alternative to liquid extraction. In these methods, the analytes are extracted from the matrix (liquid or gaseous) into non-miscible liquid or solid materials where the solutes migrate into the sorbent phase. Contrary to the extraction with adsorbents, the surface and the amount of extraction phase are very important parameters¹⁸.

The most widely used sorptive extraction phase is polydimethylsiloxane (PDMS), the most used stationary phase in GC columns due to its inertness, thermo stability and reproducibility, as well as its degradation products are well-known and easily identified by spectroscopic techniques.

It also operates under a broad temperature range (up to 320 °C) and has interesting diffusion properties, where the main interactions with solutes are Van-der-Walls type¹⁸. Nevertheless, due to some limitations for retaining the more polar analytes, other polymeric phases have been proposed for the sorption-based approaches^{12,14,17}.

1.3.1 Solid-phase extraction (SPE)

SPE is a dynamic sample preparation technique used for the enrichment, concentration and clean-up of the analytes in the analytical process, with the possibility of automation on-line with liquid chromatography (LC).

It has been applied in the studies involving environmental, biological and chemical samples, as well as in the pharmaceutical and petrochemical industries²². The advantages of this technique are the reduced analysis time, cost and labour, since SPE is faster and requires less manipulation⁹.

Recently, it has been considered a powerful alternative to liquid/liquid extraction (LLE), since it has demonstrated good precision and accuracy. The enrichment is based on the retention of the compounds from an aqueous sample on a short LC-type column (SPE cartridge), **figure 1**, followed by desorption with a suitable organic solvent. SPE is founded on the sorption of the analytes onto an active surface, instead of the partitioning equilibrium in the LLE²³. The consumption of organic solvents is significantly reduced when dealing with this technique once compared to LLE, which results in a reduced potential for formation of emulsions⁹.



Figure 1 – Schematic representation exemplifying an SPE cartridge.

1.3.2 Open-tubular trapping (OTT)

One of the first approaches that explored the properties of PDMS for sample enrichment was OTT⁵. An open-tubular trap is similar to a capillary GC column with a layer of PDMS coated onto the internal wall, **figure 2**. The sample is dynamically pumped through the OTT and the analytes present in the water sample will partition into the PDMS stationary phase³.

Thermal (TD) or liquid desorption (LD) can be performed to desorb the analytes, whereby the last one is preferred given that ensures higher sensitivity.

The advantages of using this technique are the good thermal stability, high degree of inertness and well documented retention properties. However, it never gained widespread acceptance because of several limitations, such as the excessively long sampling time, the limited sample capacity, the low amount of stationary phase per trap length and the use of longer traps to ensure adequate retentions. Additionally, it is more suitable for very nonpolar compounds since the polar ones are not retained in the thin layer of PDMS^{2,5}. Recently, a multichannel OTT was designed⁵ whereby this short trap contains several channels in parallel. However, due to the unfavourable geometry, the trap can't ensure quantitative trapping at higher flow rates (more than 15 mL/min).

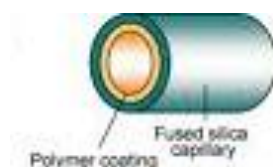


Figure 2 – Schematic representation exemplifying an OTT device.

Therefore, to overcome the presented difficulties of this extraction technique, microfluidic devices have been introduced to perform continuous liquid extraction on a miniaturized scale⁶. The extraction is based on molecular diffusion between two laminar flows formed in narrow channels, presented in 2006 by Xiao et al⁶. However, a more general approach to sample enrichment is SPE which can be easily integrated with the liquid handling capabilities of the microfluidic devices.

1.3.3 Stir bar sorptive extraction (SBSE)

SBSE is a new static sampling enrichment technique recently described by P. Sandra et al. to extract organic analytes from aqueous samples by sorption onto a thick film of PDMS on a glass-coated magnet^{18,19,22}, **figure 3**.

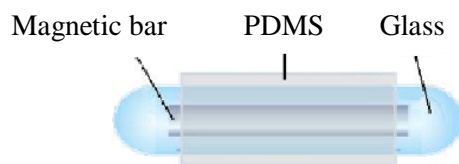


Figure 3 – Schematic representation exemplifying a SBSE device.

In SBSE the analytes of interest are extracted, under optimized conditions, by the PDMS stir bar introduced in the aqueous sample and then desorbed by TD either in a thermal unit or directly in a GC liner. Additionally, the coated bar can be also immersed in a small volume of an organic solvent which is compatible with PDMS to perform LD, followed by GC or HPLC analysis¹⁹.

Like SPME, the experimental conditions of the SBSE need to be optimized for each type of application, specifically the polarity characteristics of the analytes, the extraction time, the agitation speed, the temperature, the pH and the ionic strength with the purpose of reaching the equilibrium between both phases involved (sample and the PDMS)²².

The theory of SBSE is very similar to that of SPME, where the partitioning efficiency of the analytes into the PDMS phase of the stir bar, at equilibrium, can be reliably predicted by the octanol-water partition coefficient ($\log K_{O/W}$), because of the approximation between the partitioning coefficients of PDMS and water ($K_{PDMS} \approx K_{O/W}$), as well as by the involved phase ratio β ($= V_W/V_{SBSE}$), where V_W is the volume of the water sample and the V_{SBSE} is the PDMS volume^{19,20}. A quantitative recovery is usually reached for solutes with a $\log K_{O/W}$ value higher than 3 and an effective extraction by SBSE is also obtained for compounds with lower polarity ($\log K_{O/W} < 3$). Nonetheless, in case of incomplete extraction or non-equilibrium conditions calibration is still possible¹¹.

Although SBSE presents several advantages, such as easy manipulation with excellent reproducibility and a very good sensitivity for trace level analysis, the PDMS polymer cannot retain the more polar analytes ($\log K_{O/W} < 3$). In order to overcome this limitation, several authors have proposed new static sampling approaches, such as PDMS combined with other phases, as well as other polymers¹⁴, and bar adsorptive micro-extraction (BA μ E), operating under the floating sampling mode^{1,15}. More recently, PU have been applied as novel polymeric phases due to their sorption and mechanical properties, as well as their ease production, versatility and interesting physical and chemical properties^{2,12,14,17,25}.

PU can be defined as a plastic material which exists in various forms and is used in a broad range of commercial applications. In general, PUs are obtained by the reaction of an isocyanate and polyol (or polyalcohol) in the presence of expansion agents, catalysts and surfactants, **figure 4**, presenting soft, flexible and rigid form. The isocyanates can be aromatic or aliphatic, bifunctional or polyfunctional and the polyols are usually polyethers, polyester polyols or acrylic polyols^{16,26,27}.

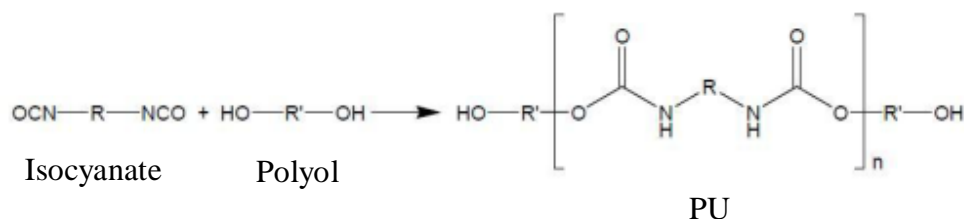


Figure 4 – Reaction scheme of the formation of PU foams.

The chemical nature along with the functionality, namely the number of reacting groups per molecule of the reagents, should be chosen in agreement with the wanted final properties. This flexibility allows obtaining materials with different physical and chemical properties, suitable for several extraction applications^{16,21,26,27}. Another property of these materials is the possibility to insert solids in the foam structure, such as adsorbents and receptors for the determination of trace metals, for instance^{21,27}.

Furthermore, PUs present appropriated sorptive and mechanical characteristics, in particular high thermal stability, simplicity and speed of synthesis and low cost^{16,26}. However, the decomposition of these polymeric phases occurs as a result of multitude physical and chemical phenomena not dominated in a single process. The study of their decomposition is particularly difficult, given that they degrade with the formation of various gaseous products where a number of decomposition steps are typically observed by thermogravimetric analysis²⁶.

These materials have been successfully applied to monitor priority compounds in environmental water samples by SBSE^{12,14}, which showed much higher selectivity and sensitivity when compared with PDMS, as well as in the headspace mode for tracing volatiles². For those reasons, the PU foams are a very attractive new generation alternative to overcome the limitation of the polymeric PDMS phase specially to recover the more polar analytes from aqueous matrices. Additionally, these polymeric phases are very resistant and regenerable materials, suitable for several dozens of analysis^{14,16}.

1.3.4 Bar adsorptive micro-extraction (BA μ E)

In order to overcome the limitations presented by the SBSE(PDMS) technology, namely the limited adsorption of the polar analytes ($\log K_{O/W} < 3$), a novel analytical approach designated by bar adsorptive micro-extraction (BA μ E) was proposed¹⁵. This analytical methodology uses powdered activated carbons, silica or alumina and polymeric materials as adsorbents phases which present surface characteristics more indicated to extract the more polar solutes.

Through the small analytical devices presenting appropriated geometry, specific sorbents are easily supported by “sticking-based technologies”. In this technique, a small plastic bar coated with appropriated sorbents is placed in the matrix operating in the floating sampling mode^{1,25,28}, **figure 5**. The devices coated with suitable adsorbents can be applied in environmental and biological matrices with the purpose of extracting the compounds of interest for posterior analysis by chromatographic and hyphenated techniques (refocus).

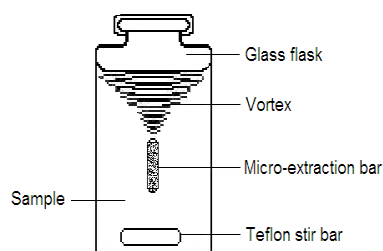


Figure 5 – Schematic representation exemplifying the BAμE device operating in the floating sampling mode.

1.4 Analytical techniques

1.4.1 Gas chromatography (GC)

Chromatography was first developed by the Russian botanist Mikhail S. Tswett in 1906, in which he obtained a colourful separation of plant pigments, specifically chlorophylls and xanthophylls, through a column of calcium carbonate^{28,29}. Since then, chromatography has been considered as a powerful tool for the separation and identification of compounds. According to IUPAC³⁰ chromatography is defined as “a physical method of separation in which the components to be separated are distributed between two phases, one of which is *stationary* while the other *moves* in a definite direction”. Therefore, the stationary phase is most commonly a viscous liquid coated on the inside of a capillary tube or on the surface of solid particles packed into the column, while the mobile phase is either a liquid or a gas³¹.

The concept of gas chromatography (GC) was first enunciated in 1941 by Martin and Synge, who were also responsible for the development of liquid-liquid partition chromatography³². In this analytical method, the sample is vaporized and injected onto the head of the chromatographic column where elution is brought about by the flow of an inert gaseous mobile phase. In contrast to most other types of chromatography, the mobile phase doesn't interact with the analytes since its only function is the transport of the analytes through the column. Gas-liquid chromatography (GLC), normally designated as GC, is based upon the partition of the analytes between the gaseous mobile phase and a liquid phase immobilized on the surface of an inert solid.

In 1955 the first commercial apparatus for GC appeared in the market and since that time this technique has been applied in several fields³².

A GC system is basically constituted by an injector, a column placed inside an oven and a detector, controlled by appropriated software. The basic components of an instrument for gas chromatography are illustrated in **figure 6**.

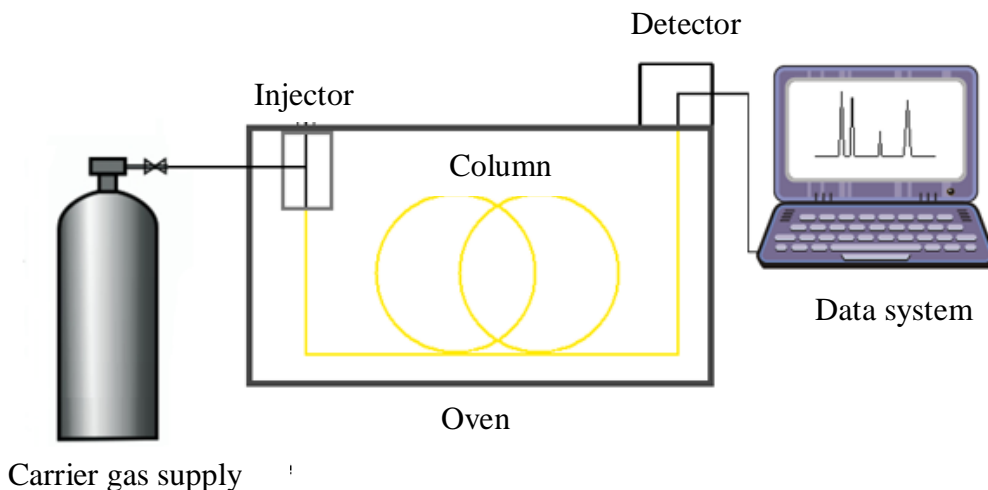


Figure 6 – Schematic representation of a typical GC system.

The carrier gas must be chemically inert and pure and includes helium, nitrogen and hydrogen. Hydrogen and helium give better resolution than nitrogen at high flow rates because the solutes diffuse more rapidly through those gases, according to the Van Deemter curve³¹. The most common method for sample injection involves the use of micro syringe to inject a liquid or gaseous sample through a self-sealing, silicone-rubber diaphragm or septum into a flash vaporizer port located at the head of the column. There are several types of sample injection, in which the most frequently used are isothermal vaporization with or without breakdown flow (split/splitless modes) and programmed temperature vaporization (PTV). In the split mode, only 0.1-5 % of the injected sample reaches the column while the remained sample is removed through a waste vent. The relation between the carrier gas from the flow controller and the flow ratio of the column (split ratio) can be responsible for the fractioning of the sample. On the other hand, for quantative and trace analysis the splitless mode is more appropriated because approximately 90 % of the sample is applied to the column and little fractionation occurs during injection³¹.

As for the PTV injection, it has the possibility of injecting large volumes (LVI) into the GC system which gives higher analytical sensitivity since it can be used to lower the detection limits of the method or to eliminate the need for concentration of extracts. The injector is designed to allow the inlet to perform a pre-separation of target analytes from solvents or other components of the sample^{28,33}. Liquid samples are injected into the PTV inlet at low temperature, where the liner is cooled down by liquid nitrogen or compressed air. During the injection and after the elimination of the solvent, through the solvent vent mode, the sample stays in the liner. Then, the temperature of the injector is rapidly increased and the analytes are transferred to the column where they can be separated and analysed.

Two general types of columns are used in GC, packed and open tubular or capillary columns, in which the last ones provide higher resolution, shorter analysis times and increased sensitivity to small quantities of analyte than packed columns, but lower capacity of sample³¹. Capillary columns, developed by Marcel Golay, are usually made of fused silica coated with polyimide (a plastic capable of withstanding 350 °C) or aluminium for support and protection from atmospheric moisture, where the stationary phase is on the inner wall of the column. The most common stationary phases are formed based on polysiloxane, where the type and percentage of the substituent groups differentiates each phase and dictates the characteristics of polarity. PDMS is the stationary phase most widely used because of its nonpolar properties. In order to fit into an oven the columns are usually formed as coils having diameters of 0.1 to 0.75 mm and 5 to 100 m of length, where they can operate in the isothermal or temperature programming modes²⁸.

The GC detector is an important device at the end of the column to detect and identify the analytes. An ideal detector must be sensitive, selective, stable and reproducible. It gives a linear response over a wide range of concentrations to the analytes under investigation. Many detectors have been investigated and used during the development of GC, among which is the flame ionization detector (FID), the thermal conductivity detector (TCD), the electron-capture detector (ECD) and the flame photometric detector (FPD)^{31,32}. The FID is the most widely used and generally applicable detector for GC, **figure 7**.

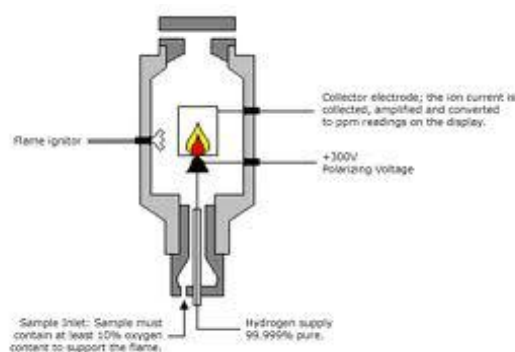


Figure 7 – Schematic representation of a typical FID.

In this detector, the effluent from the column is mixed with hydrogen and air and then ignited electrically. Most organic compounds, when pyrolyzed at the temperature of a hydrogen/air flame, produce ions and electrons that can conduct electricity through the flame. The number of ions produced is roughly proportional to the number of reduced carbon atoms in the flame³². However, because the FID responds to the number of carbon atoms entering the detector per unit of time, it is a mass-sensitive rather than a concentration-sensitive device. In addition, the detector is insensitive toward non-combustible gases such as H_2O , CO_2 , SO_2 and NO_x , making it particularly useful for the detection of pollutants in natural water samples. The detector exhibits a high sensitivity, a large linear response range and low noise and it's easy to use. On the other hand, it is a destructive detector since the samples cannot be reanalysed.

GC is often coupled with selective techniques of spectroscopy and electrochemistry, thus giving the so-called hyphenated methods that provide powerful tools to identify the compounds of complex mixtures. Gas chromatography couple to mass spectrometry (GC-MS) assumed special importance due to its advantages in terms of spectral identification, sensitivity and selectivity.

1.4.2 Gas chromatography-mass spectrometry (GC-MS)

GC-MS are, in many ways, highly compatible techniques, since the GC can separate volatile and semi-volatile compounds with great resolution and the MS can provide detailed structural information on most compounds such that they can be exactly identified³⁴.

It is the single most important tool for the identification and quantification of organic compounds in complex mixtures, being very useful for the determination of molecular weights and the elemental compositions of unknown organic compounds in those mixtures. This instrument have been used for the identification of thousands of components that are present in natural and biological systems, for instance the characterization of the odour and flavour components of foods, identification of water pollutants, medical diagnosis based on breath components and studies of drug metabolites³².

In this system, **figure 8**, the sample is introduced into the injector of a gas chromatograph, which after separation of the constituents in the column; the eluted compounds enter in the ionization chamber where they undergo ionization and fragmentation by electron impact or chemical ionization. The most common mass analyzers are the ion trap detector (ITD), quadrupole and time of flight (TOF), in which the first one is remarkably compact and less expensive. The trapped ions are then transferred from the storage area to an electron multiplier detector, which has a fast response time (of the order of nanoseconds) and the capacity of acquiring high currents, where the injection is controlled so that scanning on the basis of mass-to-charge (m/z) ratio is possible. The result is a graph (spectrum) of abundances as a function of the m/z ratios^{28,32}.

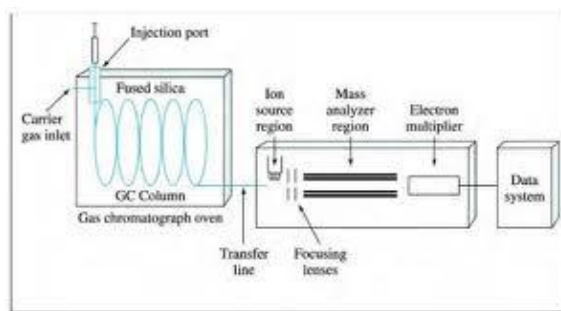


Figure 8 – Schematic representation of a typical GC-MS system.

When the mass spectrometer operates in the full-scan mode, it allows the identification of compounds from unknown samples using reference spectral libraries, such as NIST and Wiley Mass Spectral Library, among others^{28,32}.

1.4.3 Comprehensive two-dimensional gas chromatography (GC×GC)

Multi-dimensional analysis in chromatography may be considered to be any technique that combines two or more distinct separation/analysis steps, where at least one of the steps or dimensions involves a chromatographic separation³⁵. Multi-dimensional separation techniques are not confined just to analyses where there are an overwhelming number of peaks, since they are of use whenever a critical separation of compounds cannot be achieved on one column or phase type and require the use of two sequential separations on two different phase columns. Therefore, coupling two independent columns through an interface makes it an effectively way of improving the separation power of a GC system. This methodology by using a heart-cut process is capable of isolating small regions of a primary column separation and transferring them to a second column where column selectivity gives enhanced resolution of the heart-cut zone. In other words, the technique can be recommended but rapidly becomes an extremely laborious and time-consuming method, with very careful fractionation, lengthy re-analysis of all fractions and reconstruction of the chromatograms as the major problems when the main aim is screening an entire sample³⁶.

For those reasons, the alternative is to separate the entire sample on two different columns, to keep the fractions narrow in order to guarantee that the information gained during the first separation is not lost and the construction of the instrumental set-up is made as to ensure that the total 2D separation is completed within the run time of the first-dimension analysis³⁶. This process is designated by comprehensive-two dimensional gas chromatography (GC×GC) in which two GC separations based on distinctly different separation mechanisms are used with the interface, called modulator, between them, **figure 9**.

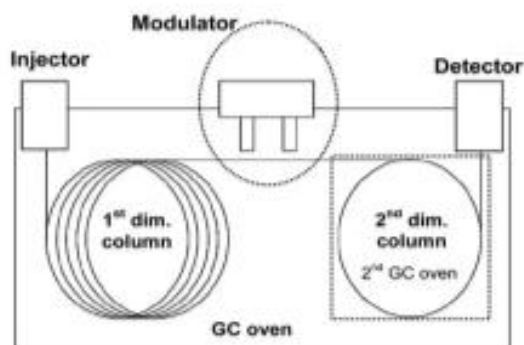


Figure 9 – Typical set-up of a GC×GC system.

The main functions of the modulator are to accumulate/trap, refocus narrow adjacent fractions of the first-column eluate and to release these rapidly into the second column^{36,37}.

In most applications, samples are first separated on a column containing a non-polar stationary phase and after modulation, each individual fraction is injected onto a much shorter, narrower column containing a (medium-) polar or shape-selective stationary phase³⁶. The most commonly detectors used in this technique are flame ionization detector (FID) and mass spectrometer (MS)³⁷.

In addition to the general benefits of a GC×GC system (sensitivity and separation enhancement), various studies have revealed other specific advantages for particular sample types, such as the separation into classes within the 2D space (for petrochemicals), the direct comparison or fingerprinting of different samples (in the case of essential oils) and the extra dimension of interference removal from target analytes (in environmental analysis)³⁵.

1.5 Aim

The present work aims to develop and apply new micro-extraction approaches for trace analysis using microfluidic devices and novel sorption based polymers, as well as acquiring experience with emerging sample preparation techniques and modern instrumental systems.

In the first part, microfluidic devices (“chips”) with different sizes and geometries will be packed with PDMS material in order to perform solid-phase extraction. The devices will then be tested in the extraction of organic analytes from aqueous matrices, using FAMES, BTEX and PAHs as model compounds. After extraction, the analytes will be desorbed using a suitable (liquid) solvent and analysed by GC-FID and GC×GC-FID.

In the second part, PUs having cylindrical geometry will be tested as innovative devices for micro-extraction using the sorption and mechanical properties of these polymers. In these studies the PUs will be soaked with suitable organic solvents and applied under the floating sampling technology and desorbed by mechanical compression followed by LVI-GC-MS(SIM) analysis. This study will be tested using priority model compounds.

Chapter 2 – Experimental

2.1 Microfluidic devices

2.1.1 Chemicals and samples

P. A. Grade ethyl acetate (EtAc, 99.5 %), methyl hexanoate (FA₆, ≥99 %), methyl octanoate (FA₈), methyl decanoate (FA₁₀, ≥97 %), methyl undecanoate (FA₁₁, ≥99%), ethylbenzene (EB, ≥99 %) and p-xylene (XY, ≥99 %) were purchased from Sigma-Aldrich (Zwijndrecht, The Netherlands). Methanol (MeOH, 99.9 %) and n-hexane (n-C₆, 99.9 %) were obtained from Biosolve (Valkenswaard, The Netherlands). Toluene (TOL, ≥99 %) was acquired from Merck (Darmstadt, Germany), while methyl laurate (FA₁₂, ≥97 %) and methyl myristate (FA₁₄, ≥99 %) were purchased from Fluka (USA). Six Polycyclic Aromatic Hydrocarbons (PAHs; naphthalene, fluorene, phenanthrene, anthracene, fluoranthene and pyrene) were obtained from Sigma-Aldrich (Zwijndrecht, The Netherlands). PDMS particles (size 0.80 mm) were obtained from Sigma-Aldrich (Zwijndrecht, The Netherlands). Ultra-pure water (18.2 MΩ cm) was obtained from an Arium 611UV Ultrapure Water Systems (Sartorius Stedim Biotech, Aubagne Cedex, France). A surface water sample was collected from the river outside the University of Amsterdam, The Netherlands. All samples were previously filtered (Whatman No. 1 filters) and stored refrigerated at 4 °C until their analysis.

2.1.2 Materials and equipment

Besides all the current laboratory equipment, conventional plastic syringe 5 mL (Once) and glass syringe [d = 23.50 mm, 50 mL]; a Kd Scientific (USA) Syringe pump, GC capillaries, frits, screws, nuts and HPLC materials (Agilent Technologies, USA), glass beads (d = 2.2 mm and 0.80 mm), glass vials of 1.5 mL (VWR International, USA) and their respective capsules, tablet press (Agilent Technologies, USA) were used.

Several microfluidic devices with different shapes and sizes were supplied by NLISIS BV (Veldhoven, The Netherlands). An HPLC pump (± 3 % RSD, Hewlett Packard, Avondale, PA, USA) was used for pressure measurements. Mass weights were determined in an analytical balance (± 0.10 mg; Mettler Toledo AG135, Switzerland).

An ultrasonic bath equipped with a thermostat (Branson® 3510 E-DTH, USA) was also used.

All one-dimensional (1D) GC and comprehensive two-dimensional GC (GC×GC) experiments were performed on an Agilent Technologies (Santa Clara, CA, USA) 6890 Series GC System equipped with a split/splitless injector, a LECO (Mönchengladbach, Germany) cryogenic modulator with secondary oven and a flame ionization detector (FID), shown in **figure 10**. The hydrogen flow for the FID was produced by a hydrogen generator PG-H2 Series 3 (Schmidlin-DBS AG, Neuheim, Switzerland). The capillary column used for GC×GC experiments was a CP-WAX (length 1.2 m, i.d. 0.10 mm, film thickness 0.20 µm) from Agilent Technologies (Germany).

All desorption efficiencies of the fractions were calculated using the formula in **appendix IV**.



Figure 10 –Gas chromatograph equipped with a flame ionization detector used for GC-FID and GC×GC-FID analysis.

2.1.3 Experimental Procedure

2.1.3.1 Preparation of the standard solutions

Individual stock solutions were prepared in MeOH at a concentration level of 440 mg/L for FA₆, FA₁₀ and FA₁₄; 540 mg/L for FA₁₁; 550 mg/L for FA₈ and 800 mg/L for FA₁₂; 88 mg/L for EB, 92 mg/L for TOL, and 100 mg/L for XY. A mixture of the six PAHs was already prepared with a concentration level of 110 mg/L in MeOH.

The FAMES test samples were prepared by spiking milli-Q water with a standard solution containing the FAMES: 0.055-0.075 mg/L for **test sample 1**; 0.055-0.075 mg/L in 5% methanol, to minimize adsorption, for **test sample 2** and 0.050 mg/L for **test sample 3** were prepared in volumetric flasks (100.0 ± 0.1) mL. Standard solutions of PAHs and BTEX at a concentration level of 0.050 mg/L were used to spike the milli-Q water. All the stock solutions were stored refrigerated at -20 °C.

2.1.3.2 GC-FID and GC×GC-FID conditions

For all the 1D GC experiments, an injector temperature of 250 °C, with a flow rate of 40 mL/min and an injection volume of 1 µL were chosen and helium was used as the carrier gas. Test samples of the FAMES were injected in the splitless mode. The oven temperature program started at 40°C (2 min) and used a heating rate of 20 °C/min to the final temperature of 320 °C.

As for the GC×GC analysis, an injector temperature of 250 °C and an injection volume of 1 µL were chosen and helium was used as the carrier gas. The PAHs and BTEX test samples were injected in the split and splitless mode at different flow rates. The oven temperature program started at 45 °C (2 min) and used a heating rate of 5 °C/min and 10 °C/min to the final temperature of 255 °C. The secondary oven and the modulator were programmed at 5 °C and 20 °C above the main oven, respectively. A modulation time of 5 seconds was chosen.

2.1.3.3 Instrumental calibration

The instrumental conditions and the method used in this thesis were already established by previous work that occurred in 2011²⁴.

2.1.3.4 Preparation of the microfluidic devices

The first chip consisted of a glass-plate (5 cm×2 cm×0.5 cm) in which a diamond-shaped metallic channel was attached, **figure 11**.

The chip had three little holes: two in each end were used as an inlet (for flushing reagents through the chip) and an outlet (connected to a collection glass flask), while the one in the middle was used to introduce the PDMS particles, (17.6 ± 0.1) mg. The chip was placed in a chip-holder, **figure 12**, and attached with a clamp to a universal holder. The plastic syringe was set on the syringe pump and connected to the chip, **figure 13**.



Figure 11 – First chip (5 cm×2 cm×0.5 cm).

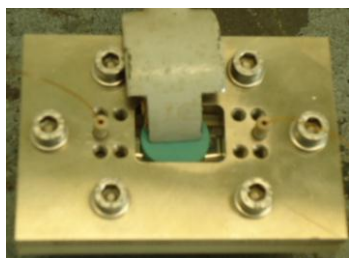


Figure 12 – Chip installed in a chip-holder.



Figure 13 – Final experimental set up of the chip.

The small LC trap (5.5 cm of length) was made with HPLC and GC materials, **figure 14 and 15**. The trap was filled with glass beads ($d = 2.2$ mm), in which (10.4 ± 0.1) mg of PDMS particles were introduced between them. All the materials used in this preparation were cleaned with MeOH, in an ultrasonic bath for 30 minutes, and the glass beads were dried in the oven, at 100 °C for 15 minutes.



Figure 14 – Materials for making the LC trap.



Figure 15 – The LC trap (5.5 cm of length).

The third chip studied was a round glass chip with no channel inside. It had two GC capillaries glued to the two little holes, in which the reagents were flushed through. The chip was packed with (10.0 ± 0.1) mg of PDMS particles through the little hole in the middle, **figure 16**.

The cylindrical glass chip (2.5 cm of length) with a channel inside had two GC capillaries glued to the little holes, **figure 17**. These capillaries were used to flush the reagents through the channel. The device was packed with (9.4 ± 0.1) mg, (14.1 ± 0.1) mg and (18.2 ± 0.1) mg of PDMS particles through a little hole on the bottom.

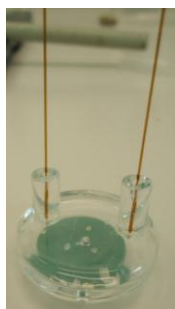


Figure 16 – Round chip with two glued capillaries and PDMS particles inside.

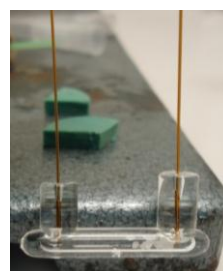


Figure 17 – Cylindrical chip with two glued capillaries and PDMS particles inside.

2.1.3.5 Performance evaluation

In a first approach, the microfluidic devices were tested in terms of leakages and flow rates, by using plastic and glass syringes (connected to a syringe pump) for flushing MeOH and milli-Q water through the chips (at flow rates ranging between 0.10 and 1 mL/min). The back pressure was also evaluated by measurements in a HPLC pump.

The drying tests were carried out under a gentle stream of nitrogen at different times (from 5 to 30 minutes) and pressure (from 0.50 to 2.5 bar). After establishing the most convenient instrumental set-ups, the performance in terms of flow rates of sample and back desorption solvent; sample volume, repeatability and desorption efficiency of the several shapes and sizes of the chips was studied.

In a typical assay, the PDMS particles (size 0.80 mm) were prepared by grinding PDMS tubing under liquid nitrogen, **figure 18**. The microfluidic chips were packed with the PDMS particles [typically $(10-18 \pm 0.1)$ mg/chip] and connected to the syringe pump and to a collection glass flask. The adsorption was performed by flushing the chip with 5 mL of MeOH and milli-Q water, followed by the test samples. Parameters such as the flow rates (four flow rate levels between 0.10 and 0.75 mL/min) and the volume (five volume levels ranging from 1 to 9 mL) of the sample were systematically studied in triplicate. The microfluidic devices were dried under a gentle stream of nitrogen.

The back-desorption was performed with EtAc, in which six flow rate levels ranging between 0.030 and 0.50 mL/min were evaluated. 125 μ L were collected into 1.5 mL vials, which were closed and placed in the automatic sampler tray for GC-FID and GC \times GC-FID analysis.

During all these studies, blank assays were also carried out with ultra-pure water without spiking and several standard controls were injected.



Figure 18 – PDMS particles used for packing the microfluidic devices (size 0.80 mm).

2.1.3.6 Application to environmental water matrices (GC×GC)

80 mL of surface water, from a river outside the University, were analysed in a GC×GC-FID system using the cylindrical chip and its optimized procedure. In this type of instrumentation some parameters were optimized such as, the inject mode (split or splitless) and flow (between 1.5 and 2 mL/min), the temperature of the primary and secondary oven and their rate (between 5 and 10 °C/min) and the acquisition delay (0 and 300 seconds). The assays were performed using the surface water without spiking; the surface water and the milli-Q water sample both spiked, with 0.050 µg/mL of BTEX and PAHs, for identification and comparison purposes.

2.2 Polyurethane foams

2.2.1 Chemicals and samples

All reagents and solvents were of analytical grade and used with no further purification. HPLC-grade methanol (MeOH, 99.9 %, Carlo Erba, Italy), acetonitrile (ACN, 99.8 %, Merck, Germany), n-hexane (n-C₆, 99.9 %, Fluka, Buchs, Switzerland), dichloromethane (DCM, 99.8 %, Carlo Erba, Italy) and ethyl acetate (EtAc, 99.5 %, Panreac, Madrid, Spain) were used. Hydrochloric acid (HCl, 34 – 37 %) was purchased from Riedel-de Haën (Germany) and sodium hydroxide (NaOH, 98.0 %) from AnalaR (BDH Chemicals, England). Atrazine (ATZ, 99.2 %), terbuthylazine (TBZ, 99.5 %) were supplied from Supelco (USA); alachlor (ALA, 99.7 %) from Riedel-de Haën (Germany) and benzo(a)pyrene [B(a)P] from Fluka (Buchs, Switzerland). PU clean-up procedures were performed according to previous report¹⁴. Ultra-pure water (18.2 MΩ cm) was obtained from Milli-Q water purification systems (USA). Surface and ground water (from a fountain and a well, respectively) were both collected in the surroundings of Lisbon (Belas, Portugal). Tap water was obtained in the metropolitan area of Lisbon and sea water from Costa da Caparica (Portugal). All samples were previously filtered (Whatman No. 1 filters) and stored refrigerated at 4 °C until their analysis.

2.2.2 Materials and equipment

Besides all the current laboratory equipment, conventional plastic syringe (5 mL, Once), high precision micro-syringes of 10 and 50 μ L (Agilent Technologies, USA), 100 and 500 μ L (Hamilton, USA), glass sampling vial of 25 mL (Variomag Multipoint, Germany) and glass vials of 1.5 mL (VWR International, Portugal) and their respective capsules, tablet press (Agilent Technologies, USA) and magnetic stir bars (VWR International, USA) were used.

Mass weights were determined in an analytical balance (\pm 0.10 mg; Mettler Toledo AG135, Switzerland). The pH was measured in a Metrohm 744 pH meter (\pm 0.01 pH value; Switzerland) and a fifteen-agitation point plate (Variomag H+P Labortechnik AG Multipoint 15, Germany) was also used.

GC-MS analysis were performed on an Agilent 6890 Series gas chromatograph equipped with an Agilent 7683 automatic liquid sampler tray and a programmed temperature vaporization (PTV), coupled to a Agilent 5973N mass selective detector (Agilent Technologies, Little Falls, DE, USA), shown in **figure 19**. The capillary column used was a HP-5MS (27.6 m \times 0.25 mm i.d., 0.25 μ m film thickness; 5 % diphenyl, 95 % PDMS) from Agilent Technologies (Germany).

The acquisition data and instrumental control were performed through the MSD ChemStation software (G1701; version C.00.00; Agilent Technologies, Germany). The identity of each compound was assigned by comparison with the mass spectra characteristics features obtained with the Wiley's library spectral data bank (G1025; Rev D.02.00; Agilent Technologies, Santa Clara, CA, USA). The recovery calculations were done by comparing the peak areas obtained from each assay with the peak areas of the standard controls used for spiking, according to the formulas presented in **appendix IV**.



Figure 19 – GC-MS system used in the present work.

2.2.3 Experimental procedure

2.2.3.1 Preparation of the standard solutions

Individual stock solutions were prepared in MeOH at a concentration level of 140 mg/L for ATZ, 230 mg/L for TBZ, 275 mg/L for ALA and in DCM at a concentration level of 265 mg/L for B(a)P. A mixture solution (10 mg/L in DCM) was prepared from the individual stock solutions of each compound in a volumetric flask.

The working and the instrumental calibration solutions were prepared by dilutions of the mixture solution at the desired concentrations and stored refrigerated at -20 °C.

2.2.3.2 GC-MS conditions

A PTV injector having a baffled liner and liquid nitrogen as inlet cooling was used. The solvent vent injection mode was performed (vent time: 0.30 min; flow: 100 mL/min; pressure: 0 psi; purge: 60 mL/min@2 min), for which the inlet temperature was programmed from 80 °C (held for 0.35 min) to 320 °C (3 min isothermal) at a rate of 600 °C min⁻¹; after reduced to 200 °C (held until the end) at a rate of 50 °C min⁻¹. The injection volume was 20 µL in the slow plunger mode. Helium as a carrier gas was maintained in the constant pressure mode (9.80 psi). The oven temperature was programmed from 80 °C (held for 1 min) at 7 °C min⁻¹ to 150 °C, then at 50 °C min⁻¹ to 280 °C (held for 5 min) in an 18.90 minutes running time. The transfer line, ion source and quadrupole analyzer temperatures were maintained at 280, 230 and 150 °C, respectively, and a solvent delay of 5 minutes was selected. In the full-scan mode, electron ionization mass spectra in the range 35-550 Da was recorded at 70 eV electron energy. In the selected-ion monitoring (SIM) mode, several groups having the target ions under study were monitored at different time windows defined by the corresponding retention times.

The instrumental sensitivity was checked by determination of the limits of detection (LOD) and quantification (LOQ) for all the compounds, obtained by the injection of diluted calibration standard solutions and calculated with a signal-to-noise (S/N) ratio of 3/1 and 10/1, respectively.

Subsequently, instrumental calibration was performed with eight concentration levels (from 1.5 to 250 $\mu\text{g/L}$) of the diluted standard solutions. All the proper dilutions were made from the mixture solution of 10 mg/L. In order to evaluate the instrumental precision, five repeated injections of each calibration level were carried out. All studies were done in triplicate.

2.2.3.3 Preparation of the PU phases

The PU foams used in this study were home-made cylinders¹⁴, as presented in **figure 20**. These foams have 1.20 g/mL of averaged density, 1 cm \times 0.5 cm of averaged dimensions and 70/80 μL of averaged volume.



Figure 20 – PU cylinders used in the present work.

2.2.3.4 Recovery assays and method validation

In a typical assay, 25 mL of ultra-pure water, spiked with the working solution at a concentration level of 1.5 $\mu\text{g/L}$, was introduced in a glass sampling vial. A PU cylinder, previously soaked in, approximately, 2 mL of DCM and n-C6, was put in the sample operating in the floating sampling mode, as shown in **figure 21**. The extraction was promoted by agitation of the magnetic stir bar for a certain period of time at room temperature (25 $^{\circ}\text{C}$). Parameters such as extraction time (15, 30, 60 and 120 min); agitation speed (750, 1000 and 1250 rpm); pH (2, 5.5, 8 and 11) with the addition of HCl 5 % and NaOH 0.01 M; organic modifier [5, 10 and 15 % of MeOH (v/v)] and ionic strength [5, 10 and 15 % of NaCl (w/v)] were systematically studied in triplicate.

For back-extraction (LD), the PU cylinder was removed with a clean tweezers, placed into a conventional syringe, **figure 22**, and compressed to a 1.5 mL vial. These assays were performed in triplicate by using several solvents (DCM, n-C6, MeOH, ACN and EtAc) and by studying the effect of the LD parameters (number of compressions and the addition of more solvent). After compressing and adding more solvent to the PU cylinder, the stripping solvent was evaporated to 200 μ L under a gentle stream of nitrogen (Ar Liquide, Portugal), in order to evaluate possible evaporation losses of the compounds. Several assays were performed and compared with non evaporated tests. The vial was closed and placed in the automatic sampler tray for LVI-GC-MS(SIM) analysis.

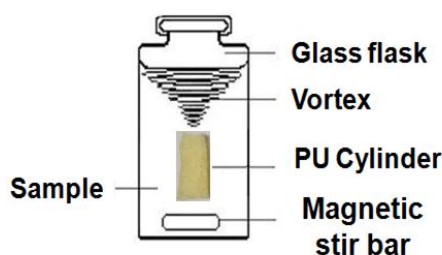


Figure 21 –Schematic representation of the PU operating in the floating sampling mode.

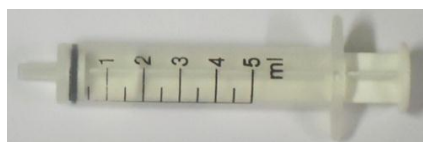


Figure 22 –Conventional plastic syringe (5 mL) used in the back-extraction step.

For the method validation experiments, 25 mL of ultra-pure water were spiked with eight concentration levels (between 0.50 and 50 μ g/L) of the diluted standard solutions, where the extraction and back-extraction assays were performed as described above under optimized conditions. Analytical limits, linear dynamic range, precision and intermediate precision were studied.

Carryover assays were also considered by injecting a standard control followed by the solvent with the intent of knowing if the compounds were retained in the capillary column.

During all these studies, blank assays were also carried out with ultra-pure water without spiking and several standard controls were injected.

2.2.3.5 Application to environmental water matrices

The standard addition methodology (SAM) was used to evaluate and suppress matrix effects on real matrices. Therefore, 25 mL of surface, ground, tap and seawater previously filtered were fortified with the compounds under study at the desire concentration (eight concentration levels between 0.50 and 50 µg/L). Blank assays (*zero-point*) were also carried out without spiking. These experiments were analyzed in triplicate using the optimized procedure described above, PUµE(DCM)-LD/LVI-GC-MS(SIM) methodology.

Chapter 3 – Results and Discussion

3.1 Microfluidic devices

3.1.1 Instrumental conditions

The GC-FID parameters, such as the retention times, were assessed in order to achieve suitable instrumental conditions for the simultaneous analysis of the model compounds under study. In a first approach, a working solution of FAMES at a concentration level of 0.050 mg/L was injected in the splitless mode. The composition of the FAMES standard solution and retention time is giving in **table 1**.

Table 1 – Composition, octanol-water partitioning coefficients ($\log K_{o/w}$), retention times (RT) of the FAMES used to evaluate the performance of the different microfluidic devices.

FAMES	Component	Log $K_{o/w}$	Solubility in water ($\mu\text{g/mL}$)	RT(min)
FA ₆	Methyl hexanoate	2.34	1400	7.71
FA ₈	Methyl octanoate	3.32	140	9.35
FA ₁₀	Methyl decanoate	4.30	14	10.79
FA ₁₁	Methyl undecanoate	4.79	4.4	11.44
FA ₁₂	Methyl laurate	5.49	1.4	12.04
FA ₁₄	Methyl myristate	6.47	0.13	13.15

The GC×GC-FID analysis was performed in qualitative terms to demonstrate that the studied microfluidic devices can be applied in a real life situations. In this case, the surface water sample collected was spiked with 0.050 mg/L of BTEX and PAHs and analysed with different parameters. The results are discussed in more detail in section 3.1.3.

3.1.2 Performance evaluation

The performance evaluation of the different microfluidic devices was assessed by preliminary tests (leakages, flow rates, back pressure, drying process and repeatability), followed by the study of sample and back extraction solvent volumes, flow rates and desorption efficiency.

The results are demonstrated for each individual chip.

3.1.2.1 First Chip

With the final experimental set up of **figure 13** the back pressure tests were performed with MeOH and water at different flow rates ranging from 0.10 to 1 mL/min. Leakages were observed when flushing water at 0.60 mL/min and higher. The back-pressure was too high because the PDMS particles move and stick together creating a block for the flow. It was observed that the high back-pressure could lead also to the formation of cracks in the glass chip. For this reason, a maximum flow of 0.50 mL/min was chosen for flushing MeOH, milli-Q water and **the test sample 1**, with a drying process of 35 minutes, under a gentle stream of nitrogen. Desorption with EtAc was performed at a lower flow rate, specifically 0.10 mL/min, and fractions of 25 μ L were collected.

Although most of the compounds are present in the first two fractions, it was observed that sometimes water was present in the first fraction. Therefore, the experiment was repeated with 45 minutes of drying.

Several extra peaks were present, **figure 23**, possibly due to impurities in the plastic syringe. Thus, the experiment was repeated using a glass syringe ($d = 23.50$ mm).

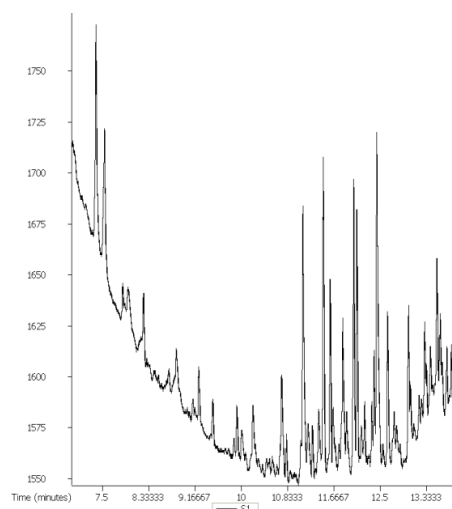


Figure 23 – Chromatogram of the first chip. Test sample 1 flushed at a flow rate of 0.50 mL/min with a plastic syringe.

However, the experiments couldn't be carried out because the PDMS particles move when solvents are flushed and they stick together. This creates a block on the entrance or the exit of the chip and generates high back-pressure on the syringe.

The problem described can be explained possibly due to the shape of the chip. By becoming narrow at the end (funnel shape) it leads to the formation of a tight blockage.

Owing to these drawbacks, a small LC column was made to be used as a trap for extracting the organic compounds, since the studied chip was not suitable for water samples.

3.1.2.2 LC trap

The first step was to measure the back pressure, in a HPLC pump, to see if this new device would give better performance than the chip previously tested, due to the linear design.

At flow rates of MeOH between 0.50-0.70 mL/min the pressure was 1 bar, but for higher flows, 0.80-1 mL/min, the pressure was 2 bar. These values were not too high to cause problems to the syringe or syringe pump.

(10.4 ± 0.1 mg) mg of PDMS particles were introduced between the glass bits, into the LC column, and the pressure was measured again to see if the PDMS would increase it. It was verified that for high flow rates, 0.50-1 mL/min, the pressure was 2 bar.

With the same set up as with the previous chip, **figure 24**, the next step was to perform MeOH and water flushing tests: 5 mL of MeOH, at 0.50 mL/min, and 10 mL of water, at 1 mL/min, were flushed through the LC column and no problems were reported.



Figure 24 – Final experimental set up of the LC column.

The device was dried with nitrogen (0.50 bar) for 15 minutes. When flushed with EtAc, at 0.50 mL/min, some droplets of water were noticed. For this reason the experiment was repeated with 30 minutes of drying. Under these conditions no more water was found in any of the fractions.

With these new developments, 5 mL of **test sample 2** were flushed, at a flow rate of 0.50 mL/min, through the trap. The experiments were performed using plastic syringes for all the flushing steps.

Nevertheless, the first fraction had some droplets of water. This indicates poor repeatability of the drying procedure. In order to avoid these problems, the drying process was increased for 45 minutes and tested at 1 and 2 bar. Even then water was observed in the fractions collected. The drawback reported could be due to the drying flow that can be very low because of the capillaries involved, **figure 15**.

Thus, a new connection to the nitrogen tube was made, **figure 25**, and a series of five drying experiments were performed at 2 bar for 30 minutes. No water was present in any of the two fractions collected for each experiment.



Figure 25 – New metal connection made to the nitrogen tube for the drying process.

Since the drying process was optimized, it was possible to test sample 2. Using a glass syringe for the desorption step with EtAc, three peaks from the apolar compounds were observed. Although the peaks were present, they were lower than expected and it was concluded that the experiment was not efficient. The compounds were probably flushed too fast and didn't have enough time to be trapped in the PDMS. Therefore, a lower flow rate of sample, 0.20 mL/min, was used. Nonetheless, the peaks were even lower than in the previous experiment which could indicate three things: loss of the compounds with the high drying pressure; compounds were not trapped efficiently due to low flow rates of sample or adsorption effects from the plastic syringes.

In order to check those possibilities, the flow rate of the sample was changed to 0.50 mL/min. Back-pressure problems were noticed when water was flushed at 1 mL/min. Consequently, the pressure was measured in a HPLC pump and at higher flow rates (0.50-1 mL/min) it was around 6-8 bar. When the apparatus was dismantled the PDMS particles were very close to the edges. This shows that they move during the experiments. One way to counter the effect was to do back flushes on the drying steps. By doing this, no more problems were found.

Even then, since the peaks continued to be very low a glass syringe was used for all the flushing steps, due to possible adsorption of the more nonpolar analytes in the plastic syringe. The experiment was performed without mechanical problems and the compounds could be identified, **figure 26**, proving therefore the existence of possible adsorption of the compounds into the plastic syringe.

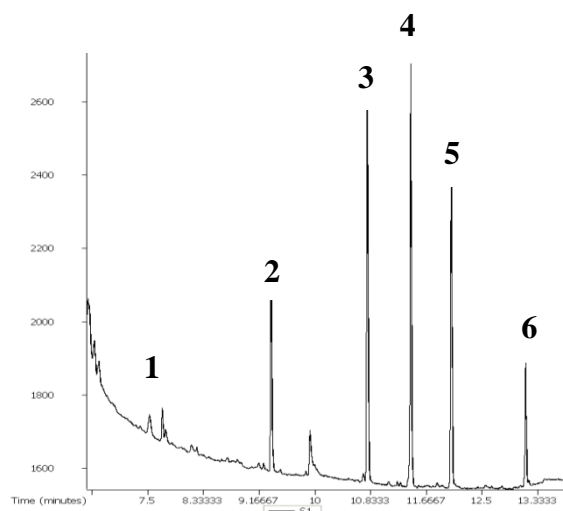


Figure 26 – Chromatogram of the LC trap. Test sample 2 flushed at a flow rate of 0.50 mL/min and back flushes on the drying steps. **1** – FA₆, **2** – FA₈, **3** – FA₁₀, **4** – FA₁₁, **5** – FA₁₂, **6** – FA₁₄.

The following parameters were evaluated under optimized conditions, such as a flow rate of 1 mL/min for flushing MeOH and water and a 30 minutes drying process under a gentle stream of nitrogen at 2 bar.

3.1.2.2.1 Flow rates of sample

The influence of flow rates of sample is a very important parameter, since it can affect the extraction yields. These experiments were performed using four flow rate levels, ranging from 0.10 to 0.75 mL/min. The results are shown in **figure 27**.

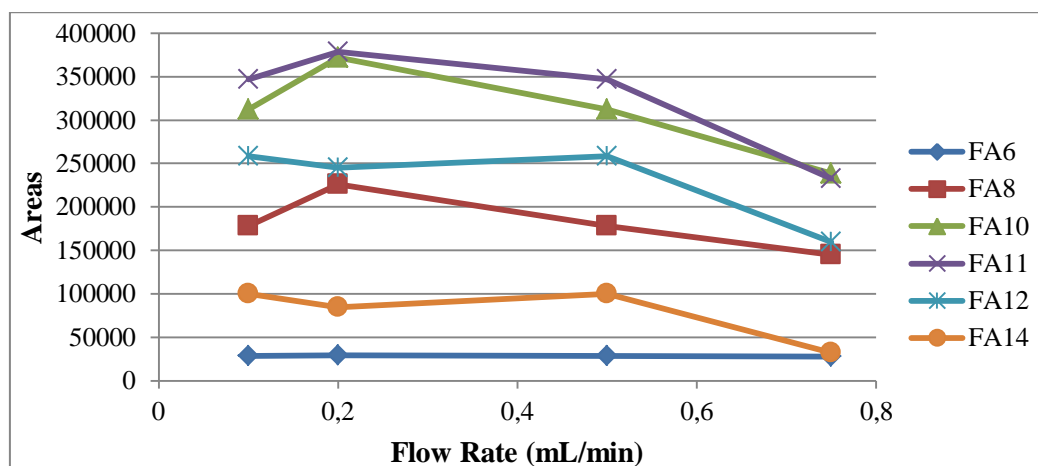


Figure 27 – The influence of different flow rates of sample (with 0.10 mL/min of flow of EtAc and 30 minutes of drying at 2 bar).

From the analysis of figure 27, in general, the areas have the tendency to decrease as the flow rate of sample increases. This indicates that at high flow rate, the compounds can't be efficiently trapped in the PDMS particles. Therefore, a flow rate of 0.20 mL/min was chosen for all following studies.

3.1.2.2.2 Repeatability

The precision was also evaluated using within – and between – day repeatability assays. The experiment was performed three times in the same day (within – day repeatability), in which the relative standard deviation, RSD (%), was calculated, **table 2**.

Table 2 – Within – day repeatability RSD values for each FAMES (at 0.20 mL/min of flow rate of sample, 0.10 mL/min of flow rate of EtAc and 2 bar of drying pressure).

Compound	RSD (%)
FA ₆	30.8
FA ₈	17.4
FA ₁₀	16.1
FA ₁₁	16.8
FA ₁₂	21.4
FA ₁₄	12.8

From these results, the RSD values are very high. This can be caused by two possibilities: the collection of the fractions isn't the same for each experiment or the drying pressure has an influence on the repeatability. To evaluate this second hypothesis, the experiments were repeated using 1 bar of drying pressure, **table 3**, in the same day.

Table 3 – Within – day repeatability RSD values for each FAMES (at 0.20 mL/min of flow rate of sample, 0.10 mL/min of flow rate of EtAc and 1 bar of drying pressure).

Compound	RSD (%)
FA ₆	5.9
FA ₈	8.6
FA ₁₀	13.3
FA ₁₁	14.1
FA ₁₂	13.9
FA ₁₄	1.8

As shown in table 3, these new RSD values are better than previous ones, indicating that the drying pressure has a significant effect on the repeatability. Therefore, 1 bar of drying pressure was chosen for the between – day repeatability studies. The assays were assessed by performing the experiment in different days, **table 4**. These results indicate that between – day repeatability is better than within – day repeatability.

Table 4 – Between – day repeatability RSD values for each FAMES (at 0.20 mL/min of flow rate of sample, 0.10 mL/min of flow rate of EtAc and 1 bar of drying pressure).

Compound	RSD (%)
FA ₆	3.3
FA ₈	0.60
FA ₁₀	0.50
FA ₁₁	0.10
FA ₁₂	0.90
FA ₁₄	0.50

3.1.2.2.3 Flow rates of EtAc

The solvent used in the back desorption process must have enough capacity to remove the compounds from the PDMS particles. Therefore, a set of experiments was performed with flow rates of EtAc ranging from 0.030 to 0.50 mL/min, **figure 28**.

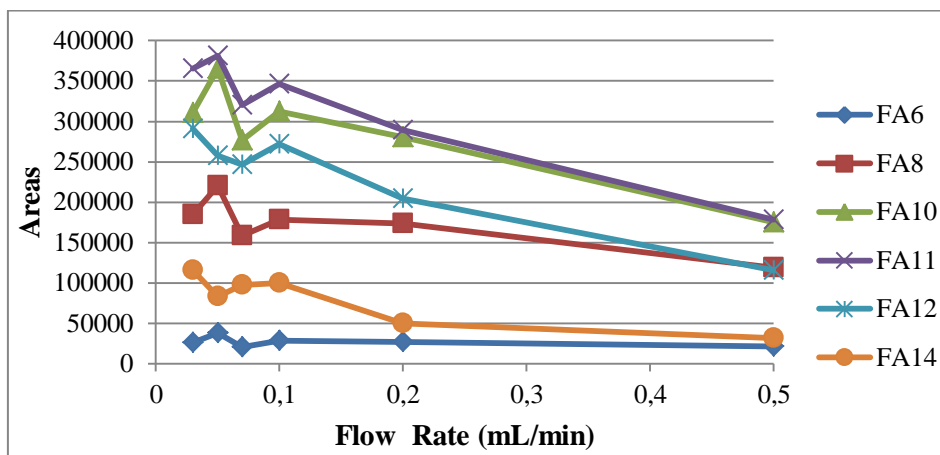


Figure 28 – The influence of different flow rates of EtAc (with 0.50 mL/min of flow rate of sample and 30 minutes of drying at 1 bar).

The results show that for higher flow rates the areas decrease, which indicates that the trapping is not efficient. From the data obtained, the parameter is not very important between 0.030 and 0.10 mL/min, but it's worse for higher flow rates. Therefore, 0.10 mL/min was used in the next experiments.

3.1.2.2.4 Desorption efficiency

The evaluation of the desorption efficiency is important to optimize the most appropriate desorption volume. The percentage was calculated for the experiments with different flow rates of sample, **figure 27**. The results are presented in **table 5**.

Table 5 – Desorption efficiencies (E) of the fractions for each FAMES at different flow rates of sample (with 0.10 mL/min of flow of EtAc and 30 minutes of drying at 2 bar).

Compound	Flow Rate (mL/min)							
	0.10		0.20		0.50		0.75	
	E _{A1} (%)	E _{A2} (%)	E _{A1} (%)	E _{A2} (%)	E _{A1} (%)	E _{A2} (%)	E _{A1} (%)	E _{A2} (%)
FA ₆	74	25	77	23	79	21	82	18
FA ₈	84	16	88	12	84	16	88	12
FA ₁₀	89	11	91	9	88	12	90	10
FA ₁₁	89	11	93	7	87	13	90	10
FA ₁₂	88	12	90	10	87	13	87	13
FA ₁₄	87	13	91	9	85	15	88	12

As can be seen, most of the analytes are recovered in the first fraction with efficiencies between 74 and 93 %. However, the nonpolar compounds are being desorbed more efficiently than the more polar compounds. The nonpolar compounds have more affinity to the PDMS and, therefore, are more difficult to desorb. On the other hand, the high drying pressure (2 bar) could be responsible for the severe losses of the more polar compounds.

3.1.2.2.5 Sample volume

The last parameter studied was the sample volume. The experiments were performed with five volume levels in between 1 and 9 mL, **figure 29**.

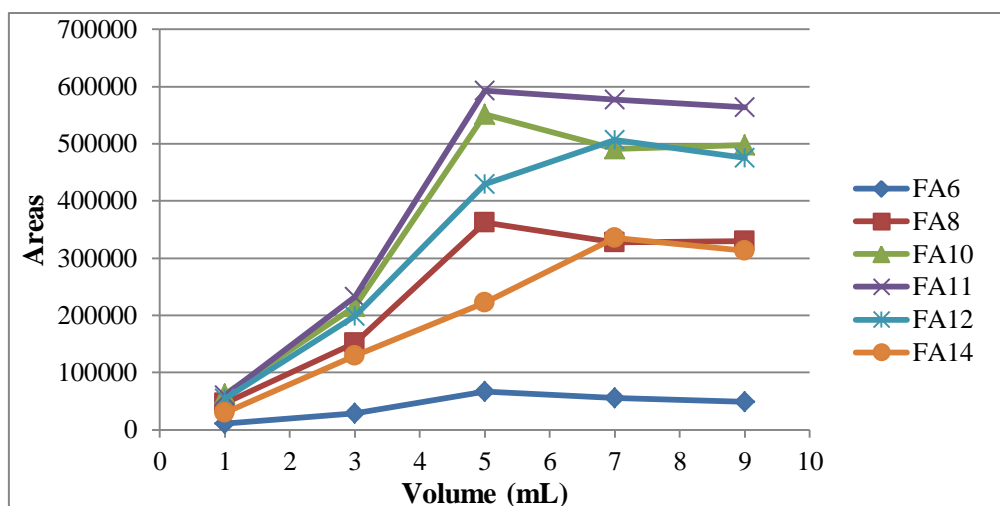


Figure 29 – The influence of volume sample (with 0.20 mL/min of flow rate of sample, 0.10 mL/min of flow rate of EtAc and 30 minutes of drying at 1 bar).

Through the analysis of the data obtained, the areas decrease for volumes higher than 5 mL. On the other hand, for volumes lower than 5 mL the linearity is acceptable, with correlation coefficients (r^2) higher than 0.9561, **figure II.1.1 – appendix II**. In light of these developments, other studies can be performed with lower concentrations of sample or with more milligrams of PDMS particles in the LC column, to improve linearity.

After all the studies reported, the optimize parameters are present in **table 6**, with desorption efficiencies of the fractions between 74 and 93 % and RSD values lower than 15 %.

Table 6 – Optimize parameters with desorption efficiencies of the fractions between 74 and 93 % and RSD values lower than 15 %.

Sample volume (mL)	5
Sample flow (mL/min)	0.20
EtAc flow (mL/min)	0.10
Drying pressure (bar)	1

3.1.2.3 Round chip

This chip doesn't have any problems with back pressure but it may not be reproducible, because of the large reservoir volume and its non linear shape, **figure 16**. Water flushing and drying tests were executed with the same final experimental set up used for the previous chip, **figure 24**.

Flushing water through the chip didn't have any problems but for the drying process with nitrogen, the chip needed to be moved to get the water closer to the inlet. Some drying processes were made in the GC oven and it was noticed that the water was disappearing little by little, after three times for 10 minutes and four times for 5 minutes at 80 °C. Since this drying process is difficult to optimize, a new set up was considered: a tip of a pipette was put inside the chip, through the bottom whole, **figure 30**. This solution proved to be very effective and the experiments with the sample (5 mL of test sample 2) could be executed.



Figure 30 – Drying system with a tip of a pipette inside the chip.

There were several peaks of impurities and no evidence of peaks of the sample, when compared to the standard, **figure 31**. The chip was cleaned and the experiment was repeated with 10 mL of sample. However, these changes didn't have any effect on the results, since there weren't any peaks of the sample.

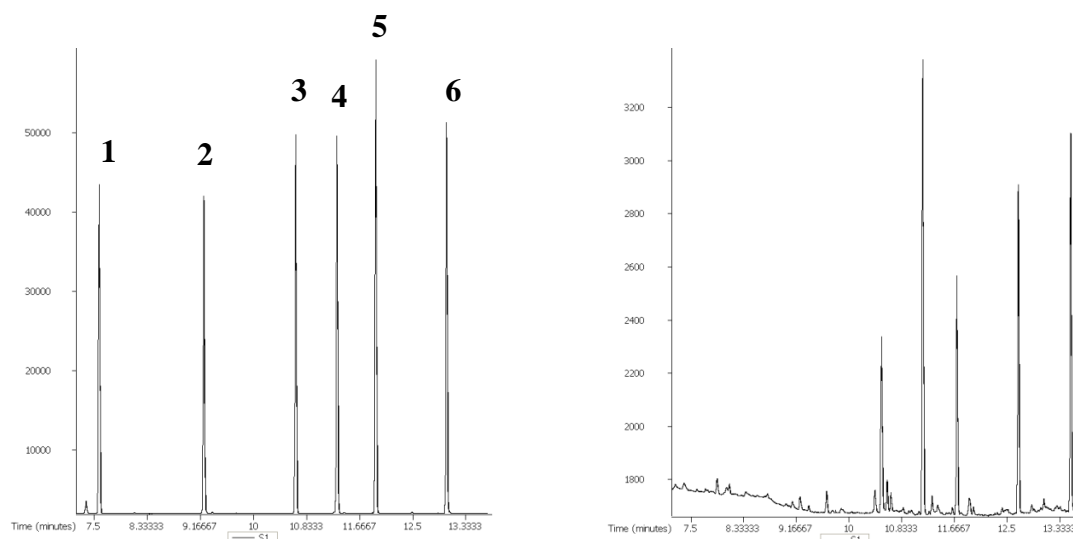


Figure 31 – Chromatogram of the standard (left) and the round chip(right) (with 0.50 mL/min of flow rate of sample, 0.10 mL/min of flow rate of EtAc and 2.5 bar of drying pressure). **1** – FA₆, **2** – FA₈, **3** – FA₁₀, **4** – FA₁₁, **5** – FA₁₂, **6** – FA₁₄.

In response to these facts, this shape is not reproducible, because the particles of PDMS move along the chip when solvents are flushed and the compounds can't be efficiently trapped.

3.1.2.4 Cylindrical chip

MeOH and water flushing and drying tests were performed, using the final experimental as **figure 24**.

A general extraction procedure for the subsequent tests was executed (10 mL at 0.50 mL/min of flow rate of test sample 2, 0.10 mL/min of flow rate of EtAc and 2 bar of drying pressure).

The nonpolar analytes are not desorbed possibly due to back desorption, indicating that the compounds stay in the PDMS particles as the EtAc is flushed. Therefore, EtAc was back flushed at a flow rate of 0.10 mL/min and the more nonpolar analyte was desorbed, namely FA₁₄, **figure 32 (number 6)**. The desorption efficiency of the second fraction is higher than expected, between 32-34 %, **figure 33**. This shows that the step of desorption is not being efficient and it's a parameter to be optimized.

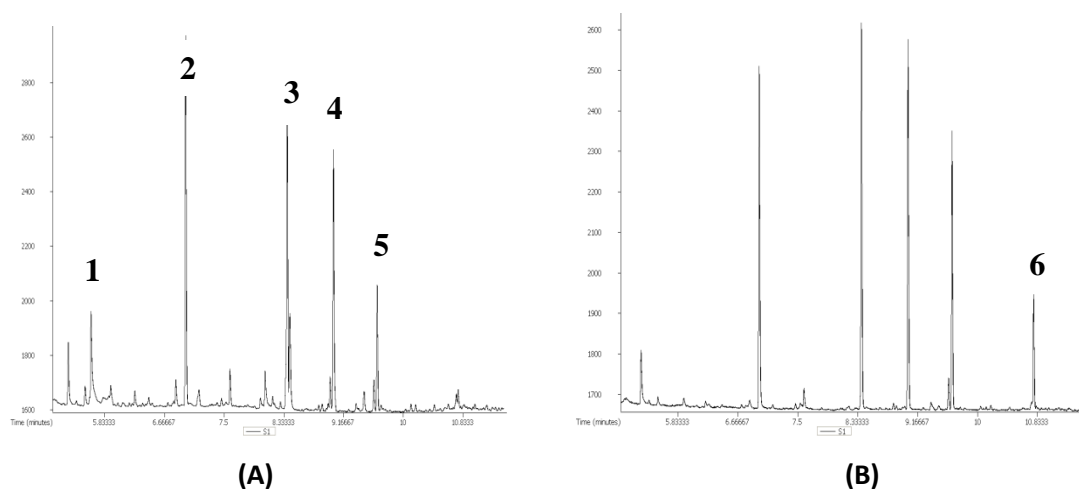


Figure 32 – Chromatogram of the cylindrical chip: EtAc flushed (**A**) and EtAc back flushed (**B**) (at 0.50 mL/min of flow rate of sample, 0.10 mL/min of flow rate of EtAc and 2 bar of drying pressure). 1 – FA₆, 2 – FA₈, 3 – FA₁₀, 4 – FA₁₁, 5 – FA₁₂, 6 – FA₁₄.

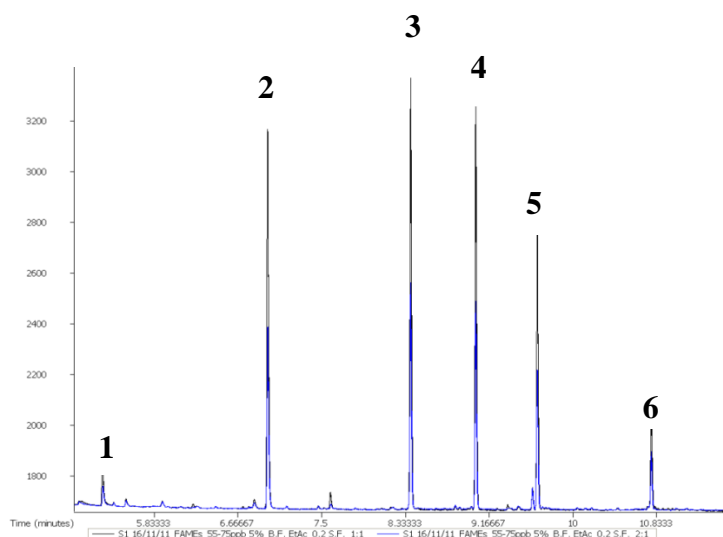


Figure 33 – Chromatogram of the cylindrical chip [(9.1 ± 0.1) mg of PDMS particles], first (black) and second fraction (blue). Efficiencies of the second fraction are 32-34%. 1 – FA₆, 2 – FA₈, 3 – FA₁₀, 4 – FA₁₁, 5 – FA₁₂, 6 – FA₁₄.

Doing the back desorption of EtAc at a flow rate of 0.020 and 0.050 mL/min the problem persisted, because the PDMS particles are not well packed due to free spaces between them.

One possible solution could be to add more PDMS particles. With (14.1 ± 0.1) mg of PDMS particles the desorption efficiency of the second fraction decreased to 21-23 %, **figure 34**, and with (18.2 ± 0.1) mg the desorption efficiency was between 9 and 11 %, **figure 35**. Therefore, (18.2 ± 0.1) mg of PDMS particles were used for the following assays.

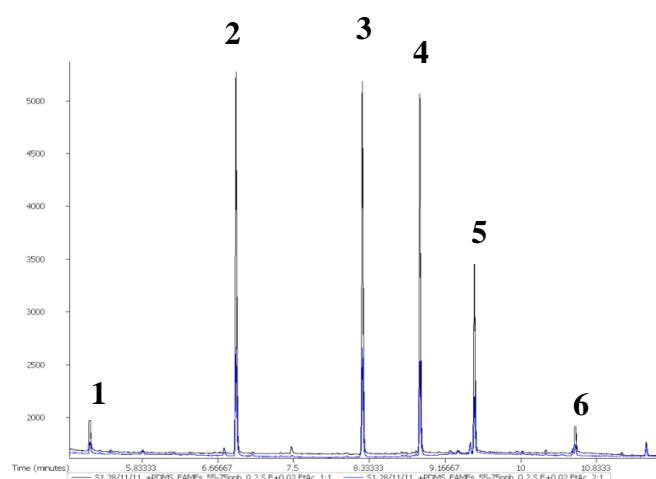


Figure 34 – Chromatogram of the cylindrical chip $[(14.1 \pm 0.1)$ mg of PDMS particles], first (black) and second fraction (blue). Efficiencies of the second fraction are 21-23%. **1** – FA₆, **2** – FA₈, **3** – FA₁₀, **4** – FA₁₁, **5** – FA₁₂, **6** – FA₁₄.

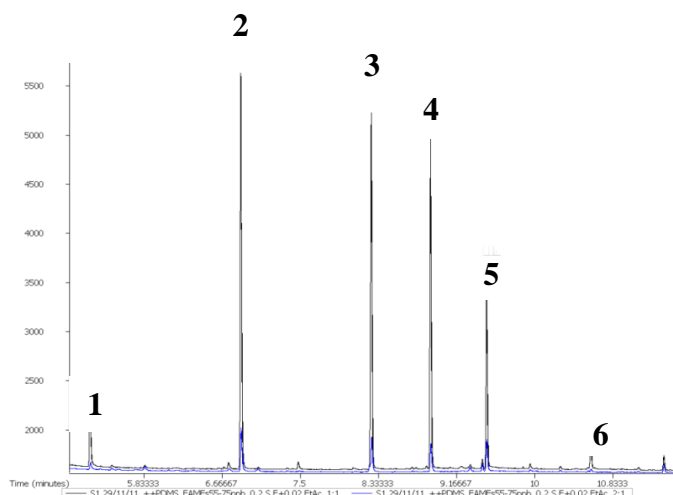


Figure 35 – Chromatogram of the cylindrical chip $[(18.2 \pm 0.1)$ mg of PDMS particles], first (black) and second fraction (blue). Efficiencies of the second fraction are 9-11%. **1** – FA₆, **2** – FA₈, **3** – FA₁₀, **4** – FA₁₁, **5** – FA₁₂, **6** – FA₁₄.

The experiment was performed three times in the same day (within – day repeatability), in which the RSD values were calculated, **table 7**.

Table 7 – Within – day repeatability RSD values for each FAMES (10 mL at 0.50 mL/min of flow rate of test sample 3, 0.020 mL/min of flow rate of EtAc back flushed and 2 bar of drying pressure, day one).

Compound	RSD (%)
FA ₆	30.5
FA ₈	25.3
FA ₁₀	23.3
FA ₁₁	26.3
FA ₁₂	25.1
FA ₁₄	16.5

These high RSD values confirm that the PDMS particles are not well packed and therefore glass beads (0.80 mm), previously dried in the oven at 100 °C for 15 minutes, were added to the chip, **figure 36**.

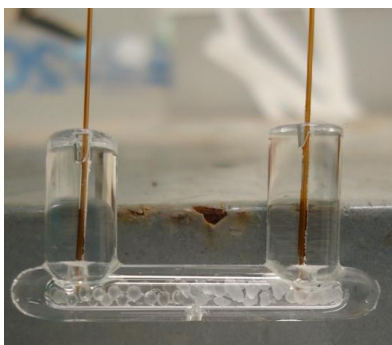


Figure 36 – Cylindrical chip with PDMS and glass beads inside.

Assays with this new set up were executed three times in the same day (within – day repeatability), in which the RSD values were calculated, **table 8**.

Table 8 – Within – day repeatability RSD values for each FAMES (10 mL at 0.50 mL/min of flow rate of test sample 3, 0.020 mL/min of flow rate of EtAc back flushed and 2 bar of drying pressure, day two).

Compound	RSD (%)
FA ₆	33.4
FA ₈	23.6
FA ₁₀	21.7
FA ₁₁	20.8
FA ₁₂	19.8
FA ₁₄	12.4

In these results, the RSD values continue to be very high, indicating that the glass beads didn't have a significant effect on the PDMS packing. Due to this reason, this shape is not efficient and repeatable because the PDMS particles can't be well packed, since they stick to the glass.

Upon the studies performed with several shapes and sizes of the microfluidic devices, the linear shape presented the best results possible, showing good repeatability (RSD between 0.50 and 15 %) and efficiencies (74-93 %). However, since the PDMS particles are very difficult to pack one possibility could be breaking them into smaller pieces or using C18 powder. Even then it's necessary to put some glass wool in the little holes to keep the C18 from blocking the capillaries.

3.1.3 Application to environmental water matrices

GC×GC analyses were performed in qualitative terms to demonstrate that the studied microfluidic devices can be applied in a real life situation. In this type of instrumentation some parameters can be optimized such as, the injection mode and flow, the temperature of the primary and secondary oven and their rate and the modulation period. It is a powerful tool since it can separate compounds that co-elute at the same retention time, being very helpful in biodiesel samples, for example.

Therefore, with the cylindrical chip and the general extraction procedure (10 mL at 0.50 mL/min of flow rate of test sample 3, 0.10 mL/min of flow rate of EtAc back flushed and 2 bar of drying pressure) a surface water sample (80 mL) was analysed in a GC×GC-FID system.

The first two parameters studied were the inlet mode and their rate: split mode with a rate of 5 °C/min and splitless mode with a rate of 10 °C/min, **figure 37**. In the splitless mode, the analytes are more visible and some co-eluted compounds were separated.

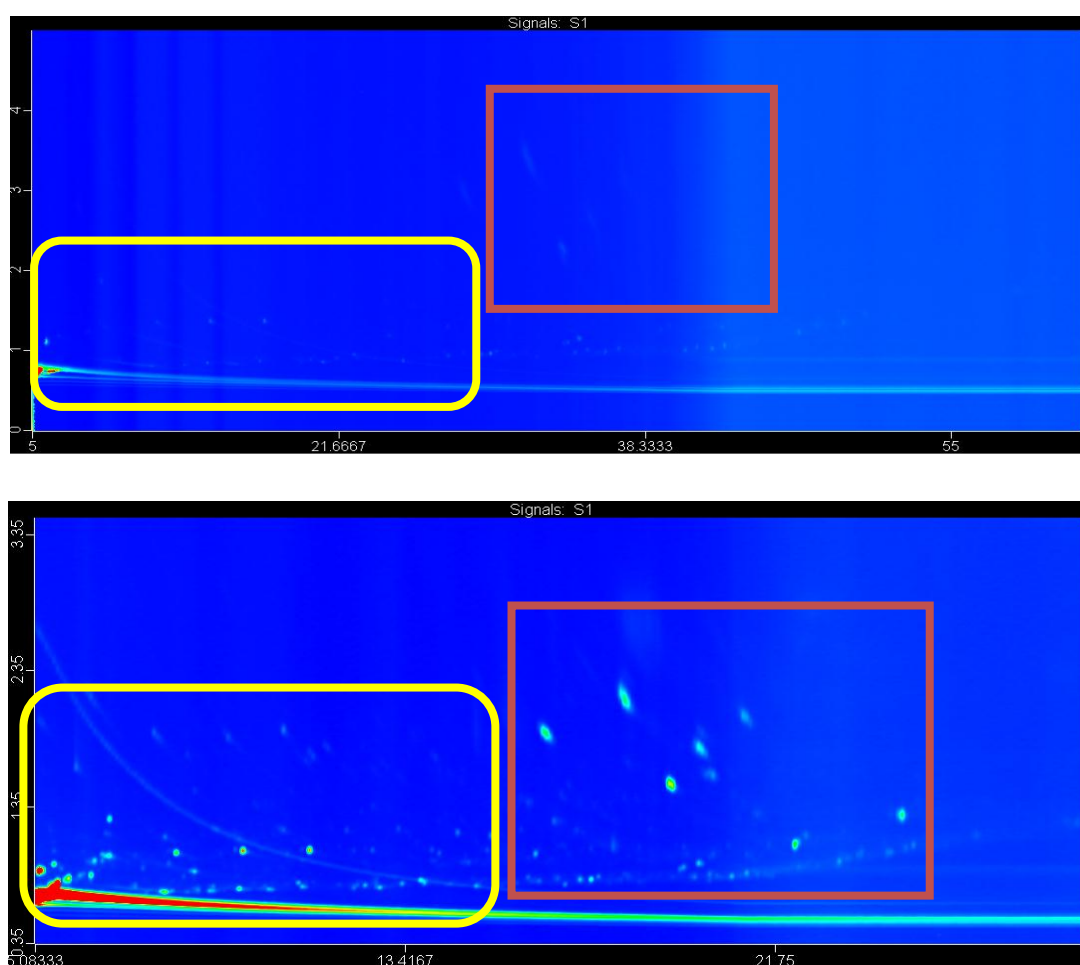


Figure 37 – 2D Chromatogram of the surface water sample, in split mode with a rate of 5 °C/min (top) and in splitless mode with a rate of 10 °C/min (bottom).

In order to identify certain compounds, BTEX and PAHs were used as standards since they have a harmful influence on the human health and are emitted into the environment from industrial processes²⁴.

For that reason, the surface water sample was spiked with 0.050 µg/mL of BTEX and PAHs. In the splitless mode, with a flow rate of 2 mL/min and an acquisition delay of 300 seconds, all the compounds are present. However, the BTEX are very difficult to distinguish and some PAHs are co-eluting.

As a result, the sample was analysed in the split mode, with a flow rate of 2 mL/min and acquisition delay of 0 seconds, **figure 38**. The chromatogram improved especially in the BTEX area.

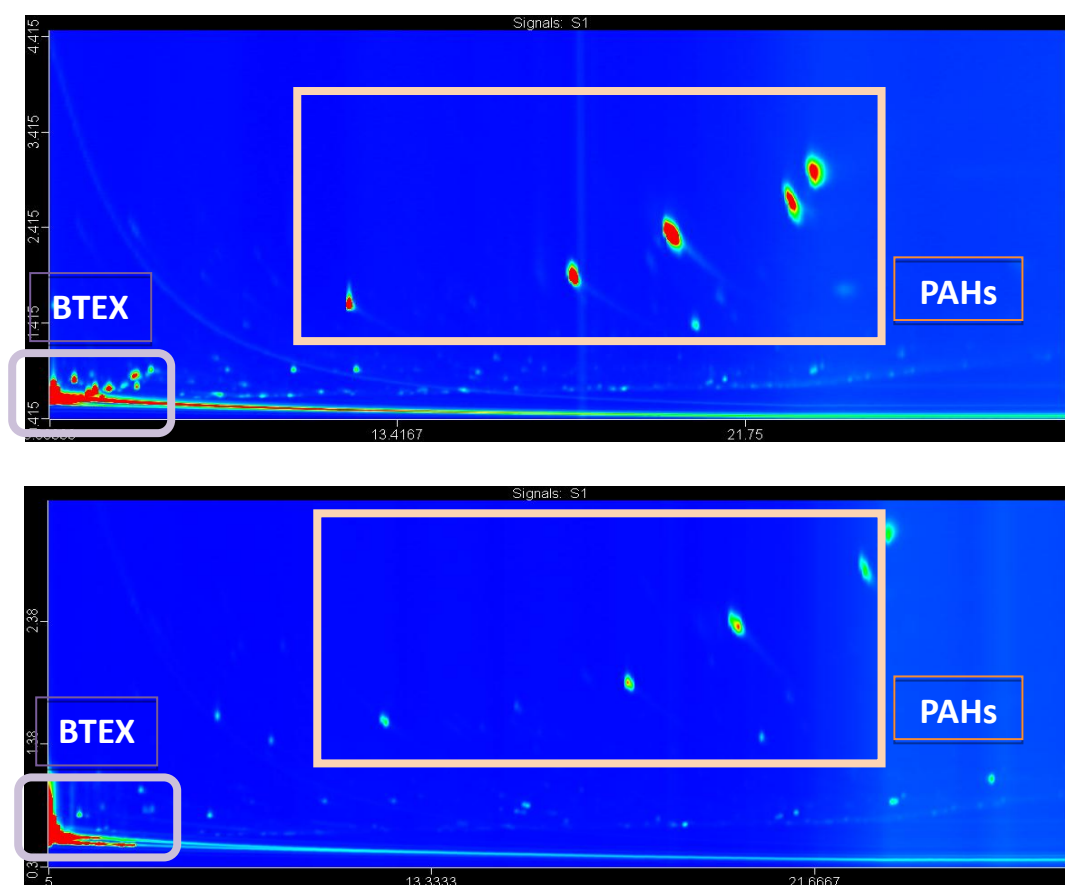


Figure 38 – 2D Chromatogram of the surface water sample spiked with 0.050 µg/mL of BTEX and PAHs, in splitless mode, a flow rate of 2 mL/min and an acquisition delay of 300 seconds (top) and in split mode, a flow rate of 2 mL/min and an acquisition delay of 0 seconds (bottom).

A clean water sample was also spiked with 0.050 $\mu\text{g/mL}$ of BTEX and PAHs to evaluate the matrix effect, **figure 39**. Several extra compounds are present in the chromatogram of the surface water sample. Those extra compounds cannot be identified because the detector is a Flame Ionization Detector (FID). Though, with a Mass Detector (MS) that could be possible.

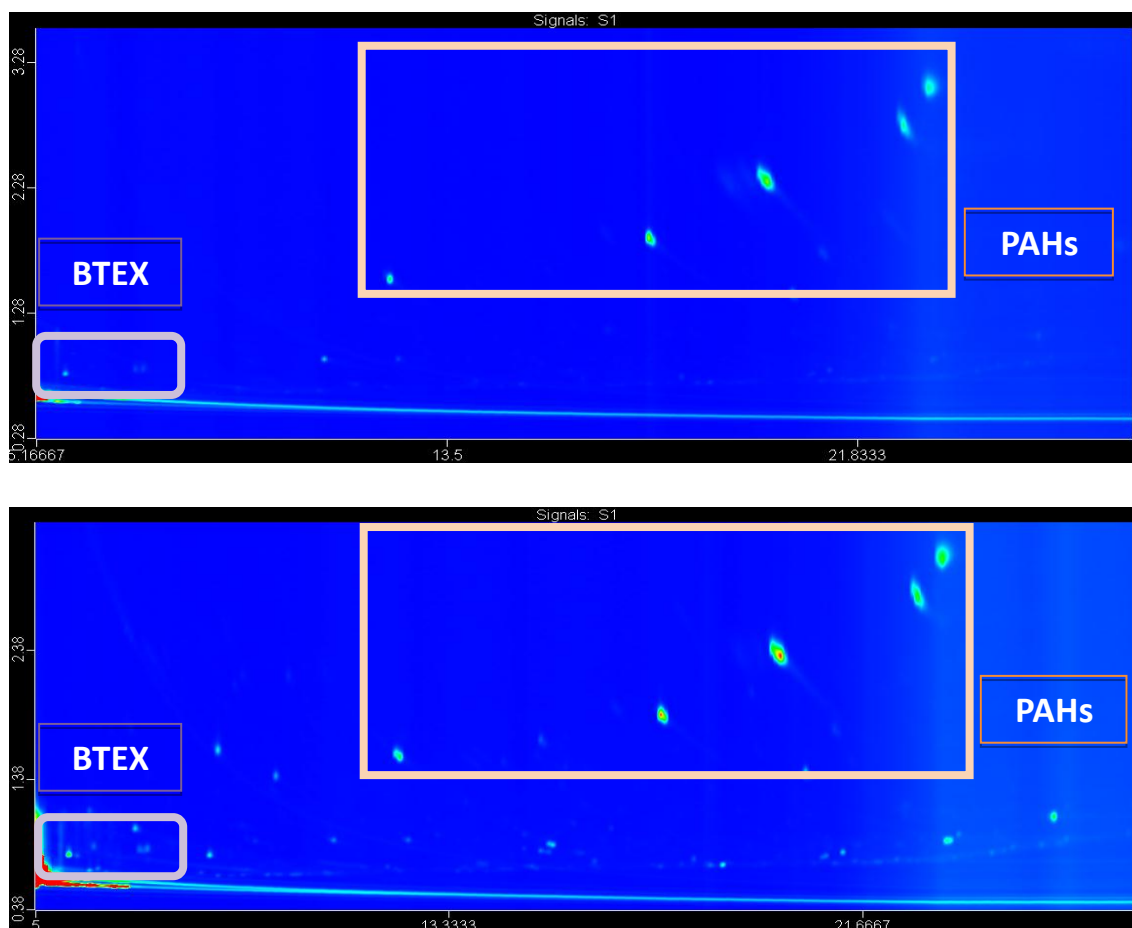


Figure 39 – 2D Chromatogram of the clean water (top) and the surface water sample (bottom) spiked with 0.050 $\mu\text{g/mL}$ of BTEX and PAHs, in split mode, with a flow rate of 2 mL/min and an acquisition delay of 0 seconds.

In more detail, three dimensional pictures, **figure 40**, show the differences between the two spiked waters better.

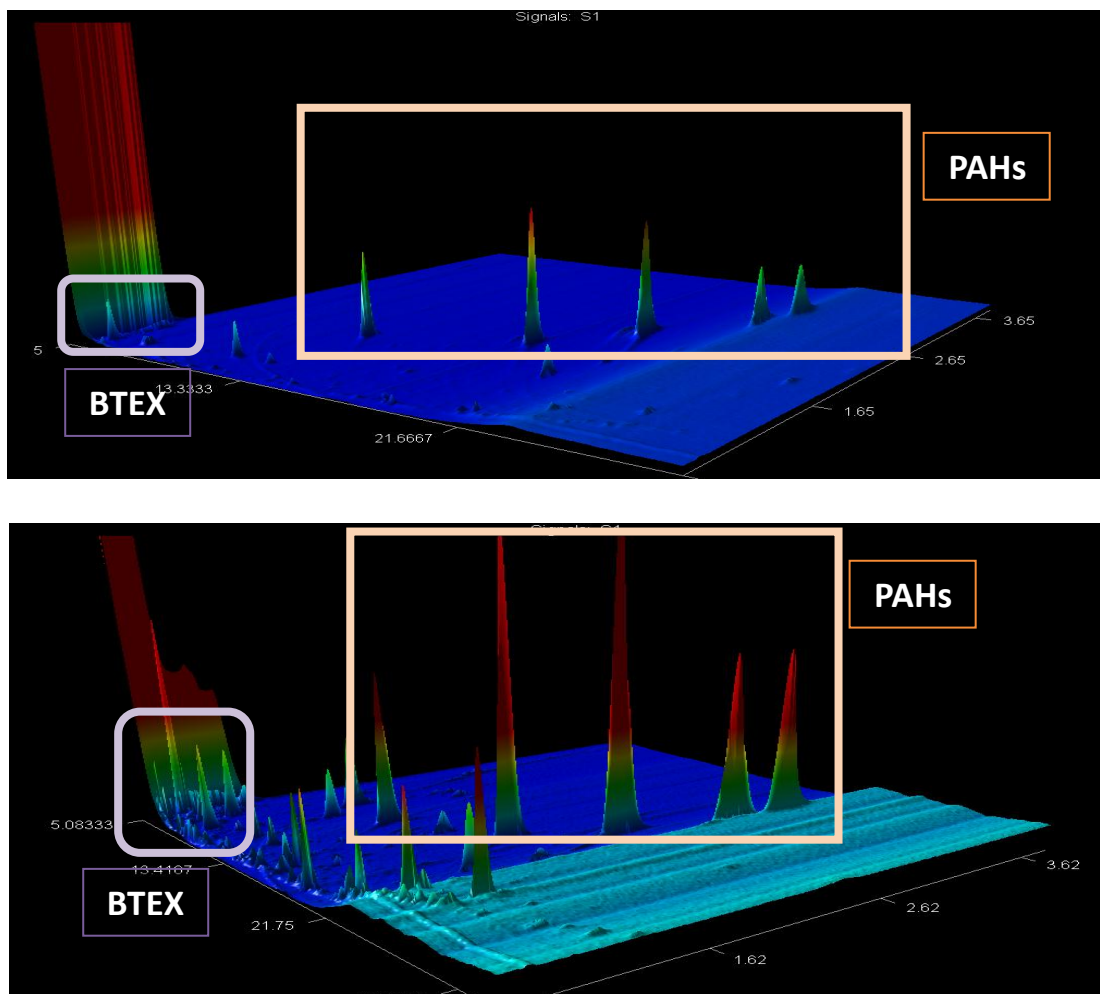


Figure 40 – 3D picture of the clean water (top) and the surface water sample (bottom) spiked with 0.050 µg/mL of BTEX and PAHs, in split mode, with a flow rate of 2 mL/min and an acquisition delay of 0 seconds.

Other studies can be performed by spiking different concentrations of the standard compounds or testing other secondary columns that can separate efficiently the co-eluting PAHs.

3.2 Polyurethane foams

3.1.1 Instrumental conditions

The GC-MS parameters, such as the retention times and the target ions, were assessed in order to achieve suitable instrumental conditions for the simultaneous analysis of the four model compounds [ATZ, TBZ, ALA, B(a)P] under study. In a first approach, a working solution at a concentration level of 500 µg/L was injected in the full-scan mode, where the target ions and their respective mass fragments of each compound were selected to facilitate their identification in the SIM mode. The spectral information regarding the selected ions, according to previous studies¹¹, is presented in the following table, **table 9**.

Table 9 – Chemical formulas, log octanol-water partitioning coefficients (log $K_{o/w}$), retention times and ions selected for quantification in SIM mode of the compounds under study.

Compound	Formula	Log $K_{o/w}$ ^(a)	pKa	rt (min)	SIM ions ^(b)
ATZ	C ₈ H ₁₄ ClN ₅	2.82	1.24	12.66	173 / <u>200</u> / 215
TBZ	C ₉ H ₁₆ ClN ₅	3.27	1.17	12.77	173 / <u>214</u> / 229
ALA	C ₁₄ H ₂₀ ClNO ₂	3.37		13.23	<u>160</u> / 188 / 268
B(a)P	C ₂₀ H ₁₂	6.11		17.05	113 / 126 / <u>252</u>
(a)	From reference number 11				
(b)	Target ion underlined.				

Under optimized GC-MS(SIM) conditions, described in section 2.2.3.2, a very good response was obtained for all four compounds, showing good sensitivity and selectivity within convenient analytical time (<20 minutes), as shown in **figure I.1.1 – appendix I**. Furthermore, to enhance sensitivity, LVI was adopted for GC-MS analysis, using injections of 20 µL, since larger volumes could lead to an increment of solvent background which can result in a lower signal-to-noise ratio²⁸.

The instrumental sensitivity was checked by determination of the limits of detection (LOD) and quantification (LOQ) for all the compounds, obtained by the injection of diluted calibration standard solutions and calculated with a signal-to-noise (S/N) ratio of 3/1 and 10/1, respectively. Values range within 0.20-2 µg/L for LODs and 0.66-6.6 µg/L for LOQs were achieved.

Subsequently, instrumental calibration was performed using eight standard solutions with concentration levels between 1.5 and 250 µg/L, in which good linear dynamic responses were observed for all the compounds with correlation coefficients (r^2) higher than 0.9956. All calibration plots are present in **figure II.2.1 – appendix II**.

Additionally, instrumental precision was also evaluated through repeated injections at two calibration levels (10 and 100 µg/L), resulting in RSDs below 4 % and no carryover effect was observed. **Table 10** summarizes all instrumental data obtained for the four compounds under study.

Table 10 – LODs, LOQs, linear dynamic ranges, correlation coefficients (r^2) and precisions (RSD) obtained by GC-MS(SIM).

Compound	LOD ^(a) (µg/L)	LOQ ^(b) (µg/L)	Linear range (µg/L)	r^2	RSD ^(c) (%)
ATZ	2.0	6.6	10 - 250	0.9984	2.9
TBZ	0.2	0.66	1.5 - 250	0.9971	2.0
ALA	0.4	1.3	2.5 - 250	0.9983	1.9
B(a)P	0.2	0.66	1.5 - 250	0.9956	3.2
(a)	S/N = 3				
(b)	S/N = 10				
(c)	Average of the two concentration levels				

3.1.2 Optimization of the PU μ E(DCM)-LD/LVI-GC-MS(SIM) methodology

The main purpose of the present work is to achieve the best experimental conditions based on a new analytical approach using PUs for extraction operating under the floating sampling technology followed by mechanical compression for the back extraction. Therefore, systematic assays were performed to optimize several parameters that are known to affect the analyte extraction^{1,14}, such as equilibrium time, agitation speed; matrix characteristics (pH, organic modifier and ionic strength) and LD conditions.

3.1.2.1 Optimization of the LD

The LD conditions that ensure complete back-extraction of the four compounds from the PU cylinder were optimized, such as the effect of evaporation, soaking and desorption solvent as well as the syringe parameters (number of compressions and volume of solvent).

3.1.2.1.1 Effect of evaporation

The evaporation of the stripping solvent is a very important concentration step, since it increases the concentration of the extract⁹. Nevertheless, this process can rouse to possible losses¹ of the more volatile compounds, such as B(a)P for the present case.

Therefore, the stripping solvent was evaporated to 200 μ L under a gentle stream of nitrogen after the compression and addition of more solvent to the PU cylinder. However, an emulsion was observed in which the water was at the upper layer and the organic solvent at the bottom.

By injecting this emulsion into the GC-MS system inconsistent recoveries were calculated, indicating poor repeatability of the method when compared to the non evaporated assays, as can be seen in **figure 41**.

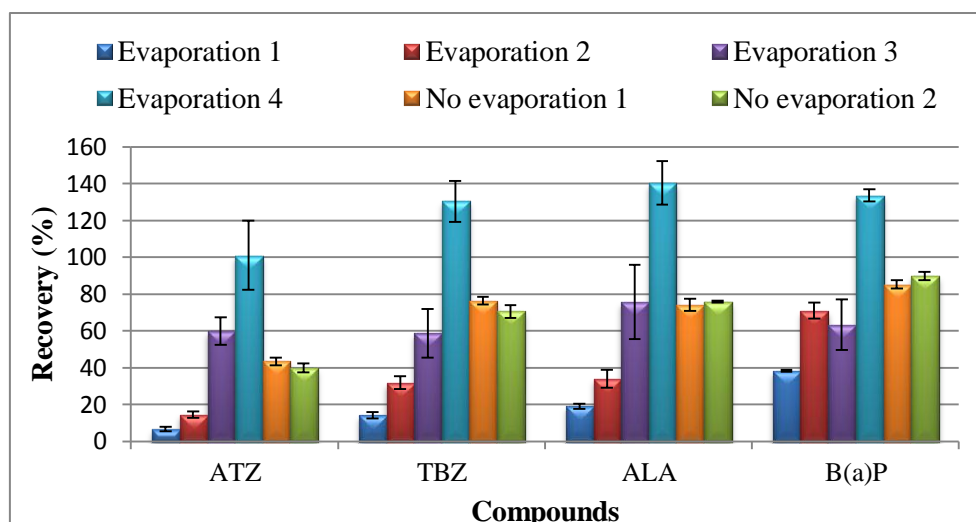


Figure 41 – Effect of the evaporation step on the average recovery of ATZ, TBZ, ALA and B(a)P (extraction: 2 h at 1000 rpm) by PU μ E-LD/LVI-GC-MS(SIM).

For that reason, the evaporation step was not performed throughout the optimization of the present methodology and all injections were done with 1 mL of the extract with the addition of some droplets of a saturated NaCl solution to better separate the emulsion.

3.1.2.1.2 Effect of the soaking and desorption solvent

The solvent must have enough capacity to promote the best recovery of all analytes from the PU cylinder²⁰. In these assays, the effect of the soaking solvent is also important because it must have the ability to desorb the analytes from the aqueous solution³⁸. Thus, experiments with the PU cylinders previously soaked with DCM and n-C6 were carried out by using DCM, n-C6, MeOH, EtAc and ACN as desorption solvents to evaluate the LD performance.

As can be seen in **figures 42** and **43**, the best soaking solvent is DCM since it presents, in general, higher recoveries when compared to n-C6.

By analysis of the different desorption solvent, DCM again shows higher recoveries (between 45 and 80 %) than n-C6 (between 1 and 16 %), MeOH (between 1 and 10 %), EtAc (between 1 and 18 %) and ACN (between 1 and 12 %), approximately. As a result, DCM was used as the soaking and the desorption solvent.

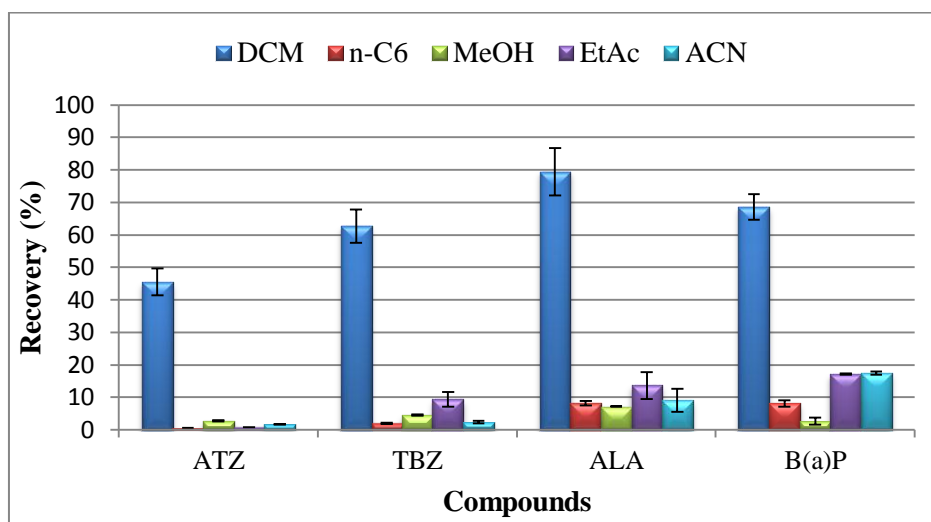


Figure 42 – Effect of the soaking (DCM) and desorption solvents on the average recovery of ATZ, TBZ, ALA and B(a)P (extraction: 2 h at 1000 rpm with the addition of some droplets of saturated NaCl solution) by PU μ E(DCM)-LD/LVI-GC-MS(SIM).

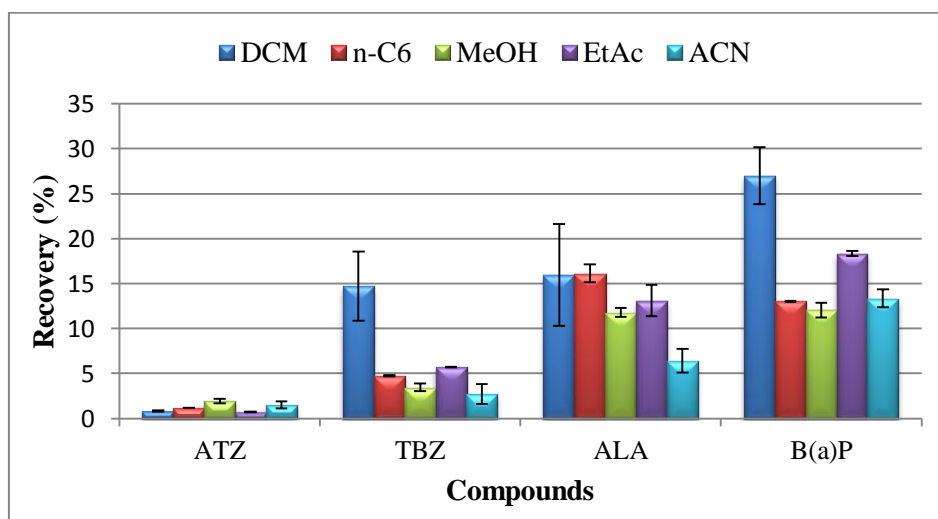


Figure 43 – Effect of the soaking (n-C6) and desorption solvents on the average recovery of ATZ, TBZ, ALA and B(a)P (extraction: 2 h at 1000 rpm with the addition of some droplets of saturated NaCl solution) by PU μ E(n-C₆)-LD/LVI-GC-MS(SIM).

3.1.2.1.3 Effect of LD parameters (number of steps)

After the selection of the most effective soaking and desorption solvents, the number of compressions performed on the conventional syringe as well as the addition of more solvent in order to increase the back extraction efficiency of the compounds were assessed.

Hence, after extraction the PU cylinder was placed into a conventional syringe and compressed for the first time (1 LD step). This procedure was repeated but for the second time (2 LD step) and the third time (3 LD step) each with 0.50 mL of DCM added to the syringe and compressed to a 1.5 mL vial. Through the analysis of **figure 44**, the 3 LD step gives the best recovery (between 15 and 70 %) when compared to the other two processes, from 0 to 3 % for the 1 LD step and from 7 to 26 % for the 2 LD step.

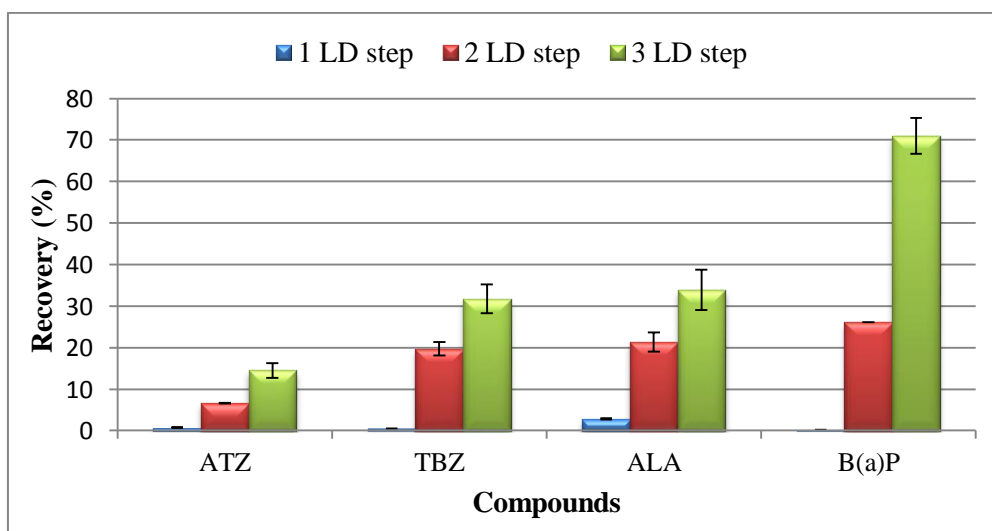


Figure 44 – Effect of the number of compressions and the addition of solvent (DCM) on the average back extraction efficiency of ATZ, TBZ, ALA and B(a)P (extraction: 2 h at 1000 rpm with the addition of some droplets of saturated NaCl solution) by PU μ E(DCM)-LD/LVI-GC-MS(SIM).

3.1.2.2 Optimization of PU μ E

Once assessed the best back extraction conditions, several extraction parameters were optimized, for instance the effect of the agitation speed, equilibrium time, pH, organic modifier (MeOH) and ionic strength (NaCl) of the matrix. The soaking solvent used in all these experiments was DCM.

3.1.2.2.1 Effect of the agitation speed

The agitation speed influences the extraction efficiency, since it controls the mass transfer or diffusion of the analytes from the aqueous media towards the polymeric phase during the sorption process¹⁴. Theoretically, the higher the stirring speed, the higher will be the mass transfer and the faster is the equilibrium achieved. However, it can decrease the extraction time but also the precision of the method^{10,28,39,40}. It must be emphasized that this parameter is very important for the floating sampling approach used in this present work.

Therefore, three stirring rates (750, 1000 and 1250 rpm) were tested using a period of extraction of 2 hours. By observation of **figure 45**, the recoveries are not influenced by the different agitation speeds, since the differences between them are negligible. Consequently, a 1000 rpm agitation speed was chosen for further experiments.

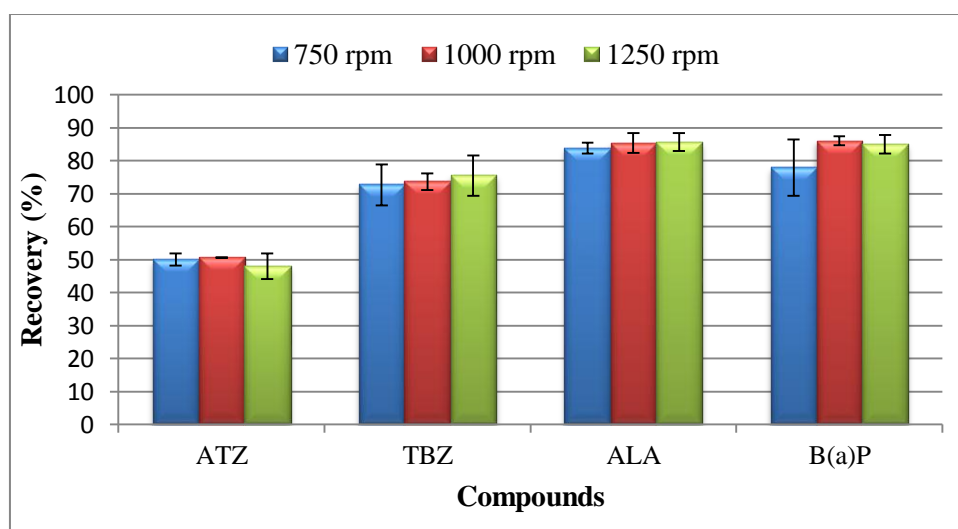


Figure 45 – Effect of the agitation speed on the average recovery of ATZ, TBZ, ALA and B(a)P (extraction: 2 h; 3 LD step with the addition of some droplets of saturated NaCl solution) by PU μ E(DCM)-LD/LVI-GC-MS(SIM).

3.1.2.2.2 Effect of the extraction time

The extraction time is related to the agitation speed as it determines the necessary equilibrium time between the analytes and the PU phase^{14,28}. Different extraction periods (15, 30, 60 and 120 min) were tested in order to establish the best compromise between time and analyte recovery, until it illustrates a constant behaviour^{28,39}.

Figure 46 shows the data obtained, where it can be observed a constant behaviour of the recovery values between 30 and 120 minutes, whereas for the former the average recovery is softly lower. Due to this fact no higher extraction periods were studied.

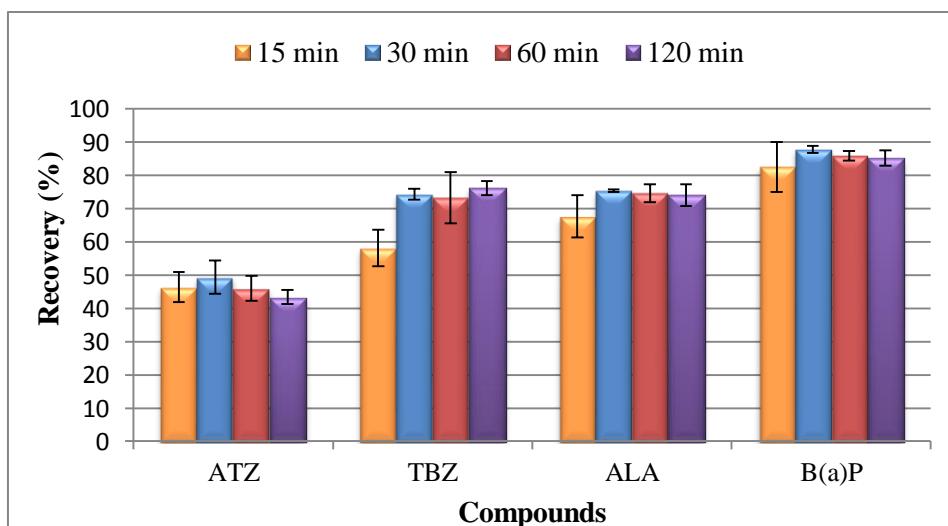


Figure 46 – Effect of the extraction time on the average recovery of ATZ, TBZ, ALA and B(a)P (extraction: 1000 rpm; 3 LD step with the addition of some droplets of saturated NaCl solution) by PU μ E(DCM)-LD/LVI-GC-MS(SIM).

Although there were no significant differences within the constant behaviour 30 minutes of extraction were selected for the subsequent studies, concluding that this analytical step is fast.

3.1.2.2.3 Effect of the pH

The effect of the matrix pH is a very important parameter to be controlled, since it can enhance the recovery of each compound by the PU cylinder. In a first approach, pH changes affect the dissociation of the triazinic molecules, where for $\text{pH} \geq 3$ ATZ and TBZ are neutral while for lower pH the molecules are protonated. The speciation of the analytes as a function of the pH, obtained by the SPARCS program, is revealed in **appendix III**.

Therefore, several values of pH were assessed (2, 5.5, 8 and 11) in order to study the effect on the recovery yields, **figure 47**.

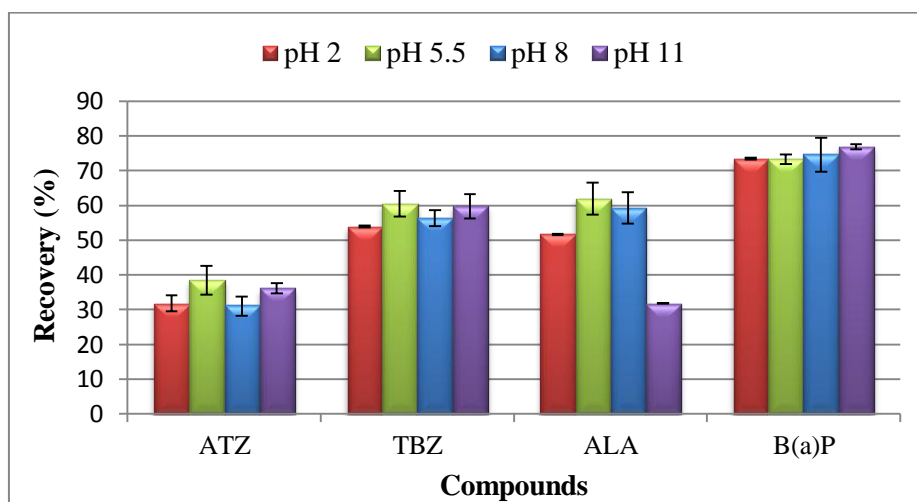


Figure 47 – Effect of the pH in the matrix on the average recovery of ATZ, TBZ, ALA and B(a)P (extraction: 30 min at 1000 rpm; 3 LD step with the addition of some droplets of saturated NaCl solution) by PU μ E(DCM)-LD/LVI-GC-MS(SIM).

Through the results obtained, the pH value of 5.5 promotes the best recoveries for the four compounds. Other pH values cause lower recovery for all analytes in general; the exception is B(a)P where the recovery is not pH dependent.

Additionally, for ALA the recovery decreases with high values of pH due to possible degradation of the polymeric phase in a more basic medium, since this analyte doesn't ionize, **appendix III**.

3.1.2.2.4 Effect of an organic modifier

One phenomenon that occurs when dealing with the more hydrophobic compounds is their possible adsorption onto the walls of the glass sampling flasks, designated by “wall-effect”. As a consequence, analyte losses and decreased recovery yields can be observed^{11,14,20}. However, sometimes it depends on the state of the glass surface, which could be damaged by abrasive cleaning materials or strong acids²⁰. Thus, the addition of an organic solvent is able to minimize this negative effect, since adding small amounts of MeOH or ACN can slightly increase the solubility of the more nonpolar compounds in aqueous media, causing higher recovery values^{20,41}. Therefore, assays were performed through the addition of several contents of MeOH (0, 5, 10 and 15 %; v/v) in the aqueous matrix.

From the analysis of **figure 48**, maximum recovery yields are obtained in the absence of MeOH in the matrix and the progressive addition of the organic solvent reduces significantly the recovery of the compounds, in general.

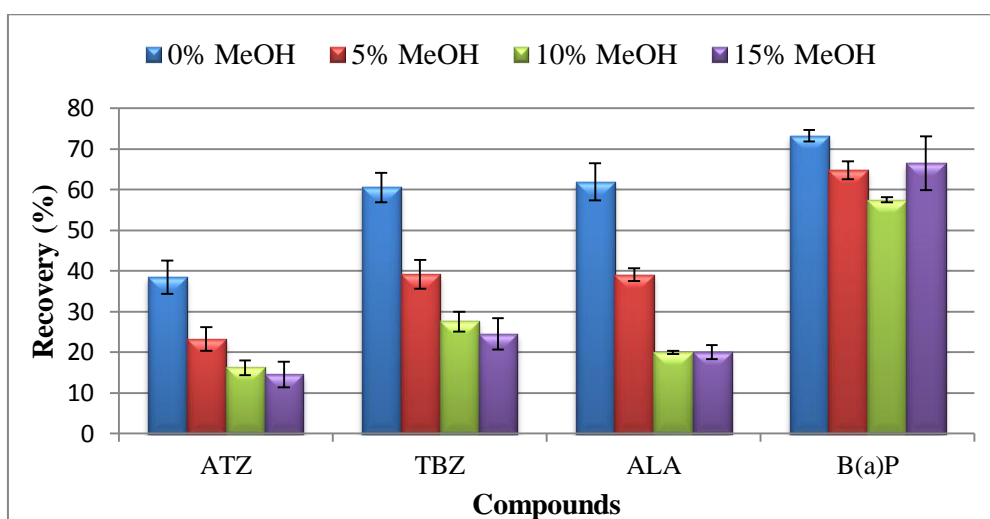


Figure 48 – Effect of the addition of an organic modifier (MeOH) on the average recovery of ATZ, TBZ, ALA and B(a)P (extraction: 30 min at 1000 rpm, pH of 5.5; 3 LD step with the addition of some droplets of saturated NaCl solution) by PU μ E(DCM)-LD/LVI-GC-MS(SIM).

This evidence can be explained by the fact that MeOH turns the matrix less polar and promotes the better solubilisation of the hydrophobic compounds in the aqueous medium, reducing their affinity towards the polymeric phase, specifically for B(a)P¹⁷. Also, another possible explanation could be the fact that the soaked PU with DCM could be the dissolution into the matrix with MeOH. In other words, higher contents of MeOH in the aqueous medium can promote ease dissolution of the DCM, reducing therefore, the extraction capacity of the polymeric phase.

Consequently, the next studies were carried out without MeOH in the matrix.

3.1.2.2.5 Effect of the ionic strength

The ionic strength effect is controlled by the addition of NaCl to the matrix and it is another factor that has a great influence on the extraction efficiency of this type of methodology^{25,39}. However, it's very important for compounds that have a log $K_{O/W}$ lower than 3, since it promotes the “salting out” effect. Namely, the presence of an electrolyte will cause a decrease in the solubility of the more polar compounds in order to increase their affinity to the polymeric phase and therefore increase their recovery.

Hence, the effect of several concentrations of NaCl (0, 5, 10 and 15 %; w/v) in the aqueous medium was evaluated. **Figure 49** shows this effect, where the presence of NaCl causes, in general, higher average recoveries for all the compounds. However, for ATZ and TBZ no significant differences were observed between 5 and 15 % of salt, while for ALA the recovery decreases as the concentration of salt increases. One possible explanation could be the occupation of the superficial area of the polymeric phase with the salt ions that blocks the interaction between the PU phase and the compound¹⁴. Nevertheless, for B(a)P the salt addition does not affect the recovery.

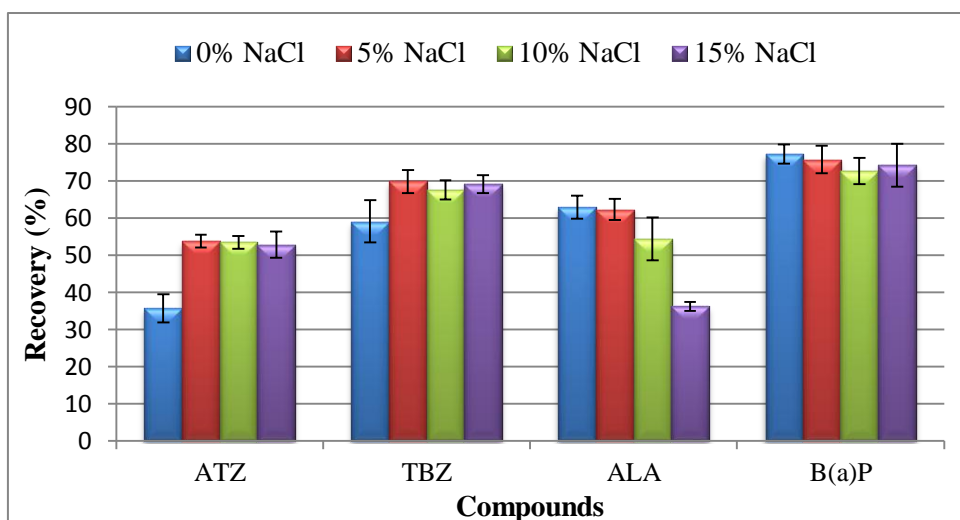


Figure 49 – Effect of the ionic strength (NaCl) on the average recovery of ATZ, TBZ, ALA and B(a)P (extraction: 30 min at 1000 rpm, pH of 5.5, 0 % of MeOH; 3 LD step with the addition of some droplets of saturated NaCl solution) by PU μ E(DCM)-LD/LVI-GC-MS(SIM).

As a result, 5 % of NaCl was chosen for being the best compromise for the target compounds, since it increased the recovery of ATZ and TBZ and had no considerable influence on the rest of the analytes.

3.1.3 Validation of PU μ E(DCM)-LD/LVI-GC-MS(SIM) methodology

After studying the most important parameters that could affect the PU μ E(DCM)-LD efficiency, a set of optimized conditions was established, **table 11**. The recoveries obtained under these conditions ranged between 50 and 75 %, **table 12**.

Table 11 – Summary of the optimized conditions established for PU μ E(DCM)-LD/LVI-GC-MS(SIM) methodology.

Optimized Conditions		
Extraction	Soaking solvent	DCM
	Extraction Time (min)	30
	Agitation speed (rpm)	1000
	pH	5.5
	MeOH (%)	0
	NaCl (%)	5
Back extraction	Evaporation	No
	Desorption solvent	DCM; 2×0.50 mL
	Number of compressions	3

Table 12 – Average recoveries of the target compounds obtained under optimized conditions by PU μ E(DCM)-LD/LVI-GC-MS(SIM) methodology.

Compounds	Recovery (%)
ATZ	50.1 \pm 6.7
TBZ	71.5 \pm 6.3
ALA	67.0 \pm 9.7
B(a)P	75.2 \pm 2.2

The assessed optimized conditions were applied for further experiments, such as the analytical validation and the application to environmental water matrices, performed in triplicate. In a first approach, the method performance, particularly the analytical limits (LOD and LOQ) of the methodology, the method calibration and the precision were evaluated. Therefore, assays under optimized conditions were conducted on ultra-pure water matrices spiked at several concentration levels.

The sensitivity of the methodology was verified through the LOD and LOQ achieved for all the four target compounds and measured with a (S/N) ratio of 3/1 and 10/1, respectively. Values ranging from 0.080 to 0.50 μ g/L for LODs and between 0.26 and 1.65 μ g/L for LOQs were achieved, **table 13**.

Table 13 – Analytical limits (LOD and LOQ) for the studied compounds obtained by PU μ E(DCM)-LD/LVI-GC-MS(SIM), under optimized conditions.

Compound	LOD ^(a) (μ g/L)	LOQ ^(b) (μ g/L)
ATZ	0.25	0.83
TBZ	0.080	0.26
ALA	0.080	0.26
B(a)P	0.50	1.65
(a)	S/N = 3	
(b)	S/N = 10	

The LODs achieved are a consequence of the better recovery yields obtained through the PU phase. They represent a lack of sensitivity particularly to be in compliance with the international regulatory directives on water quality, since the European Union directive in drinking water quality (98/83/CE) establishes 0.10 μ g/L as the maximum concentration level for individual pesticides and 0.50 μ g/L for the sum of them. Nevertheless is in compliance with other types of water^{14,42,43}.

Subsequently, the method calibration was assessed using eight concentration levels ranging from 0.50 to 50 μ g/L, in which good linear dynamic responses were observed with correlation coefficients (r^2) higher than 0.9937, **table 14**. The calibration plots are presented in **figure 50**, in which the proposed methodology shows much higher sensitivity to B(a)P, once a greater slope is obtained.

Table 14 – Parameters of the method calibration [linear dynamic range, slope (a) and correlation coefficients (r^2)] obtained by PU μ E(DCM)-LD/LVI-GC-MS(SIM) for the four model compounds, under optimized conditions.

Compound	Linear range (μ g/L)	a	r^2
ATZ	1.0 - 50	177029	0.9937
TBZ	0.50 - 50	267512	0.9981
ALA	0.50 - 50	54855	0.9987
B(a)P	2.5 - 50	917574	0.9985

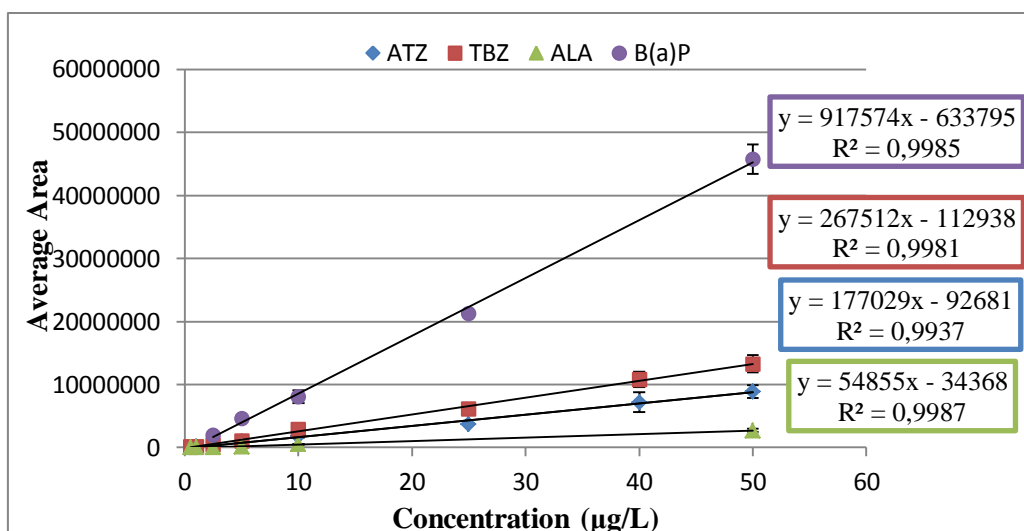


Figure 50 – Calibration plots for the four compounds obtained by PU μ E(DCM)-LD/LVI-GC-MS(SIM) methodology, under optimized conditions.

Furthermore, the precision was also evaluated using within – and between – day repeatability. For the within – day repeatability assays, the RSD values were calculated for five replicates at two concentration levels (5 and 40 µg/L), while for the between – day repeatability tests only one concentration level (25 µg/L) was used. For the proposed method, a RSD value below 25 % was achieved in compliance with the requirements of Directive 98/83/EC for trace analysis of organic compounds⁴⁴. **Table 15** demonstrates that the calculated RSD values are below 8 %, which shows to be in good agreement with those requirements.

Table 15 – Precision parameters, within – and between – day repeatability, RSD (%), obtained by PU μ E(DCM)-LD/LVI-GC-MS(SIM) methodology, under optimized conditions.

Compound	RSD (%) ^(a)	RSD (%) ^(b)
ATZ	3.0	6.8
TBZ	2.1	4.4
ALA	3.4	0.90
B(a)P	3.1	5.2
^(a)	within-day repeatability	
^(b)	between-day repeatability	

Additionally, no carry-over effects were noticed using series of replicates and the method has proven to be robust.

3.1.4 Application to environmental water matrices

In order to evaluate the applicability of the proposed methodology, assays on real matrices, including surface, ground, tap and seawater samples, were performed using the SAM approach to account intrinsic contamination and possible matrix effects. Therefore, the matrix was fortified with five working standards to produce the corresponding spiking levels (5-40 µg/L) for the target compounds. Blank assays (*zero-point*) were also executed without spiking to ensure maximum control of the analytical methodology.

The regression plots of the water samples, **appendix II.3**, showed good linear dynamic responses with correlations coefficients (r^2) higher than 0.9932, except for ALA ($r^2 = 0.9838$). Nevertheless, no matrix effects were observed because the c_0 was below the LODs achieved for all the compounds under study. **Table 16** presents the regression parameters, such as the slope (a) and the correlation coefficients (r^2).

Table 16 – Regression parameters obtained from SAM, under optimized conditions, for the water matrices studied using ATZ, TBZ, ALA and B(a)P as model compounds.

	Surface water		Ground water		Tap water		Seawater	
Compounds	a	r^2	a	r^2	a	r^2	a	r^2
ATZ	112116	0.9954	102637	0.9992	93780	0.9939	65303	0.9934
TBZ	196767	0.9955	165177	0.9968	161945	0.9969	114170	0.9962
ALA	32722	0.9932	47610	0.9980	11629	0.9838	9594.7	0.9968
B(a)P	451791	0.9967	375856	0.9987	328916	0.9977	213938	0.9979

Chapter 4 – Conclusions and Future Work

The present work aimed to develop and apply new micro-extraction approaches for trace analysis using microfluidic devices and novel sorption based polymers.

In the first part, microfluidic devices (“chips”) with different sizes and geometries were studied in dynamic mode and applied in the extraction of FAMES, BTEX and PAHs used as model compounds in aqueous media. The linear shape presented the best data, showing good repeatability ($0.50 < \text{RSD} \leq 15\%$) and efficiencies (74-93 %), by using 5 mL of sample at a flow sampling rate of 0.20 mL/min, 1 bar of drying pressure of nitrogen and a 0.10 mL/min flow rate of EtAc for LD. The other devices were not reproducible or efficient because the PDMS particles move when solvents were flushed and couldn't be well packed, since the particles stick to the glass. However, due to the difficulty of packing the PDMS particles, the application of the methodology in aqueous matrices, surface water in particular, was performed in qualitative terms in order to demonstrate that these microfluidic devices could be applied in real life situations. These studies were evaluated by using GC×GC-FID, which demonstrated to be a useful tool for this type of analysis. Nevertheless, other studies can be performed by spiking different concentrations of the standard compounds or testing other secondary columns that can separate efficiently the co-eluting PAHs.

In order to overcome these packing difficulties, the future work could be to break the PDMS particles into smaller pieces or using C18 powder. Even then it's necessary to put some glass wool in the little holes of the microfluidic device avoiding that the C18 blocks the capillaries.

In the second part, PUs having a cylindrical geometry were applied as innovative devices for micro-extraction using the sorption and mechanical properties of these polymers. Therefore, a novel approach using PUs soaked with convenient solvents was applied operating in static mode under the floating sampling technology. From the solvent evaluation assays, DCM proved to be the more efficient soaking solvent. Although the LD using the mechanical compression approach of the polymers demonstrated a good performance, the addition of more solvent is needed for a better back extraction.

The optimization of the proposed methodology combined with a LVI-GC-MS(SIM) system showed the best conditions for extraction: 30 min, 1000 rpm, pH 5.5 with the addition of 5 % of NaCl. For back-extraction, mechanical compression of the PU cylinder one time; two times 0.50 mL of DCM were added and compressed again to a 1.5 mL vial, with the addition of some droplets of saturated NaCl solution to avoid emulsion. Under optimized conditions, recovery yields between 50 and 75 % were obtained in ultra-pure waters spiked at the 1.5 µg/L level.

Furthermore, the validation of the method showed good linearity ($r^2 > 0.99$), in the concentration range of 0.50 and 50 µg/L, and RSD values below 10 %, where the LODs and LOQs achieved were in between 0.080-0.50 µg/L and 0.26-1.65 µg/L, respectively.

The application of this methodology to real matrices, including surface, ground, tap and seawater samples using the standard addition method, showed good analytical performance ($r^2 > 0.99$), where no matrix effects were observed.

For future work, the proposed methodology could be applied in other matrices, such as food (*e.g.* wine) and biological (*e.g.* urine) samples. Also, the sensitivity can be improved by changing some parameters of the micro-extraction and/or the instrumental set up in order to lower the LODs and LOQs values. For instances, by increasing the sample volume to 50 mL or the amount of PU phase (higher superficial area). For example, the LVI amount could be changed to 50 µL, although higher (S/N) ratios could occur.

Chapter 5 – Bibliography

- [1] N. R. Neng, A. S. Mestre, A. P. Carvalho, J. M. F. Nogueira, “Powdered activated carbons as effective phases for bar adsorptive micro-extraction (BA μ E) to monitor levels of triazinic herbicides in environmental water matrices”, *Talanta*, 83 (2011) 1643 – 1649.
- [2] C. Rodrigues, F. C. M. Portugal, J. M. F. Nogueira, “Static headspace analysis using polyurethane phases – Application to roasted coffee volatiles characterization”, *Talanta*, 89 (2012) 521 – 525.
- [3] Erik Baltussen, Frank David, Pat Sandra, Hans-Gerd Janssen, Carel A. Cramers, “Sorption tubes packed with polydimethylsiloxane: A new and promising technique for the preconcentration of volatiles and semivolatiles from air and gaseous samples”, *J. High Resol. Chromatography*, Vol. 21, June 1998.
- [4] Erik Baltussen, Frank David, Pat Sandra, Hans-Gerd Janssen, Carel A. Cramers, “Retention model for sorptive extraction-thermal desorption of aqueous samples: application to the automated analysis of pesticides and polyaromatic hydrocarbons in water samples”, *Journal of Chromatography A*, 805 (1998) 237 – 247.
- [5] Erik Baltussen, Pat Sandra, Frank David, Carel Cramers, “Stir bar sorptive extraction (SBSE), a novel extraction technique for aqueous samples: theory and principles”, *J. Microcolumn Separations*, 11(10) (1999) 737 – 747.
- [6] J. P. Kutter, Stephen C. Jacobson, J. Michael Ramsey, “Solid phase extraction on microfluidic devices”, *J. Micro Sep.*, Vol 12, October 1999.
- [7] E. Baltussen, C. A. Cramers, P. J. F. Sandra, “Sorptive sample preparation – a review”, *Anal. Bioanal. Chem.*, 373 (2002) 3 – 22.
- [8] B. V. Burger, M. Le Roux, B. Marx, S. A. Herbet, K. T. Amakali, “Development of second-generation sample enrichment probe for improved sorptive analysis of volatile organic compounds”, *Journal of Chromatography A*, 1218 (2011) 1567 – 1575.

- [9] Somenath Mitra, "Sample Preparation Techniques in Analytical Chemistry", John Wiley & Sons Inc. Publication, New Jersey, **2003**.
- [10] Maria de Fátima Alpendurada, "Solid-phase micro-extraction: a promising technique for sample preparation in environmental analysis", *Journal of Chromatography A*, 889 (**2000**) 3 – 14.
- [11] P. Serôdio, J. M. F. Nogueira, "Multi-residue screening of endocrine disrupters chemicals in water samples by stir bar sorptive extraction-liquid desorption- capillary gas chromatography-mass spectrometry detection", *Analytica Chimica Acta*, 517 (**2004**) 21 – 32.
- [12] Fátima C. M. Portugal, Moisés L. Pinto, João Pires, J. M. F. Nogueira, "Potentialities of polyurethane foams for trace level analysis of triazinic metabolites in water matrices by stir bar sorptive extraction", *Journal of Chromatography A*, 1217 (**2010**) 3707 – 23710.
- [13] A. Prieto, O. Zuloaga, A. Usobiaga, N. Etxebarria, L. A. Fernández, "Development of a stir bar sorptive extraction and thermal desorption-gas chromatography-mass spectrometry method for the simultaneous determination of several persistent organic pollutants in water samples", *Journal of Chromatography A*, 1174 (**2007**) 40 – 49.
- [14] Fátima C. M. Portugal, Moisés L. Pinto, J. M. F. Nogueira, "Optimization of polyurethane foams for enhanced stir bar sorptive extraction of triazinic herbicides in water matrices", *Talanta*, 77 (**2008**) 765 – 773.
- [15] N. R. Neng, A. R. M. Silva, J. M. F. Nogueira, "Adsorptive micro-extraction techniques – Novel analytical tools for trace levels of polar solutes in aqueous media", *Journal of Chromatography A*, 1217 (**2010**) 7303 – 7310.
- [16] N. R. Neng, M. L. Pinto, J. Pires, P. M. Marcos, J. M. F. Nogueira, "Development, optimisation and application of polyurethane foams as new polymeric phases for stir bar sorptive extraction", *Journal of Chromatography A*, 1171 (**2007**) 8 – 14.

- [17] Ana Rita M. Silva, Fátima C. M. Portugal, J. M. F. Nogueira, “Advances in stir bar sorptive extraction for the determination of acidic pharmaceuticals in environmental water matrices. Comparison between polyurethane and polydimethylsiloxane polymeric phases”, *Journal of Chromatography A*, 1209 (2008) 10 – 16.
- [18] Frank David, Pat Sandra, “Stir bar sorptive extraction for trace analysis”, *Journal of Chromatography A*, 1152 (2007) 54 – 69.
- [19] Carlo Bicchi, Chiara Cordero, Patrizia Rubiolo, Pat Sandra, “Impact of water/PDMS phase ratio, volume of PDMS and sampling time on Stir Bar Sorptive Extraction (SBSE) recovery of some pesticides with different $K_{O/W}$ ”, *J. Sep. Sci.*, 26 (2003) 1650 – 1656.
- [20] C. Almeida, J. M. F. Nogueira, “Determination of steroid sex hormones in water and urine matrices by stir bar sorptive extraction and liquid chromatography with diode array detection”, *Journal of Pharmaceutical and Biomedical Analysis*, 41 (2006) 1303 – 1311.
- [21] H. J. M. Bowen, “Adsorption by polyurethane foams; New method of separation”, *J. Chem. Soc. A*, 1970.
- [22] C. Almeida, P. Rosário, P. Serôdio, J. M. F. Nogueira, “Novas perspectivas na preparação de amostras para análise cromatográfica”, *Boletim da Sociedade Portuguesa de Química*, 95 (2004) 69 – 77.
- [23] Erik Baltussen, Hans-Gerd Janssen, Pat Sandra, Carel A. Cramers, “A novel type of liquid/liquid extraction for the preconcentration of organic micro pollutants from aqueous samples: Application to the analysis of PAHA’S AND OCP’s in water”, *J. High Resol. Chromatography*, Vol. 20, July 1997.
- [24] D. Peroni, et al., *J. Chromatogr. A* (2011), doi: 10.1016/j.chroma.2011.08.001.
- [25] Tese de Mestrado de Rute Sequeiros: *Aplicação de novas metodologias analíticas no estudo de compostos fenólicos em matrizes alimentares*, 2009.
- [26] D. K. Chattopadhyay, Dean C. Webster, “Thermal stability and flame retardancy of polyurethanes”, *Progress in Polymer Science*, 34 (2009) 1068 – 1133.

- [27] V. A. Lemos, M. S. Santos et al, “Application of polyurethane foam as a sorbent for trace metal pre-concentration – A review”, *Spectrochimica Acta Part B*, 62 (2007) 4 – 12.
- [28] Tese de Doutorado de Nuno Neng: *Desenvolvimento de novas metodologias analíticas conducentes à monitorização de poluentes orgânicos prioritários em matrizes aquosas*, 2011.
- [29] <http://www.umich.edu/~orgolab/Chroma/chromahis.html> (Agosto de 2012).
- [30] L. S. Ettre, “Nomenclature for Chromatography (IUPAC Recommendations 1993)”, *Pure & Appl. Chem.*, Vol. 65, No. 4, (1993) 819 – 872.
- [31] D. C. Harris, “Quantative Chemical Analysis”, 6th edition, W. H. Freeman, New York, 2003.
- [32] D. A. Skoog, E. J. Holler, S. R. Crouch, “Fundamentals of Analytical Chemistry”, 8th edition, Thomson Brooks/Cole, Canada, 2004.
- [33] Don Clay, Rollen Anderson, “Large Volume Injections with Programmed Temperature Vaporizing Injector for Gas Chromatography”, *Thermo Electron Corporation*, Italy, 2004.
- [34] Frank A. Settle, “Handbook of Instrumental Techniques for Analytical Chemistry”, Prentice Hall, England, 1997.
- [35] Philip Marriot, Robert Shellie, “Principles and applications of comprehensive two-dimensional gas chromatography”, *Trends in Analytical Chemistry*, Vol. 21, No. 9 + 10 (2002) 573 – 583.
- [36] M. Adahchour, J. Beens, R. J. J. Vreuls, U. A. Th. Brinkman, “Recent development in comprehensive two-dimensional gas chromatography (GC×GC). I. Introduction and instrumentl set-up”, *Trends in Analytical Chemistry*, Vol. 25, No. 5 (2006) 438 – 454.
- [37] M. Adahchour, J. Beens, R. J. J. Vreuls, U. A. Th. Brinkman, “Recent development in comprehensive two-dimensional gas chromatography (GC×GC). II. Modulation and detection”, *Trends in Analytical Chemistry*, Vol. 25, No. 6 (2006) 540 – 552.

- [38] Projeto Tecnológico de Isabela Silva: *Aplicação de Espumas de Poliuretano como fases poliméricas inovadoras em Técnicas Analíticas de micro-extração*, **2011**.
- [39] Tese de Mestrado de Carlos Almeida: *Otimização da extração sorptiva em barra de agitação com desorção líquida e análise por HPLC/DAD na determinação de hormonas esteroides em matrizes ambientais e biológicas*, **2005**.
- [40] Kiyokatsu Jinno, Masahiro Taniguchi, Makiko Hayashida, “Solid phase micro extraction coupled with semi-microcolumn high performance liquid chromatography for the analysis of benzodiazepines in human urine”, *Journal of Pharmaceutical and Biomedical Analysis*, 17 (**1998**) 1081 – 1091.
- [41] A. Peñalver, V. García, E. Pocurull, F. Borrull, R. M. Marcé, “Stir bar sorptive extraction and large volume injection gas chromatography to determine a group of endocrine disrupters in water samples”, *Journal of Chromatography A*, 1007 (**2003**) 1 – 9.
- [42] European Communities (Drinking Water) Regulations, No.2, **2007**.
- [43] Shang-Da Huang, Hsin-I Huang, Yu-Hsiang Sung, “Analysis of triazine in water samples by solid-phase micro-extraction coupled with high-performance liquid chromatography”, *Talanta*, 64 (**2004**) 887 – 893.
- [44] Official Journal of the European Communitie: *Council Directive 98/83/EC*, **1998**.
- [45] Site wikipedia (Agosto de 2012)
- [46] Maria Filomena Camões, “A água do mar tem tudo”, *Boletim da Sociedade Portuguesa da Química*, 101 Abril/Junho **2006**.
- [47] Erik Baltussen, Hans-Gerd Janssen, Pat Sandra, Carel A. Cramers, “A new method for sorptive enrichment of gaseous samples: Application in air analysis and natural gas characterization”, *J. High Resol. Chromatography*, Vol. 20, July **1997**.
- [48] Heleni Tsoukali, Georgios Theodoridis, Nikolaos Raikos, Ifigeneia Grigoratou, “Solid phase micro-extraction gas chromatographic analysis of organophosphorus pesticides in biological samples”, *Journal of Chromatography B*, 822 (**2005**) 194 – 200.

- [49] R. F. Alves, A. M. D. Nascimento, J. M. F. Nogueira, “Characterization of the aroma profile of Madeira wine by sorptive extraction techniques”, *Analytica Chimica Acta*, 546 (2005) 11 – 21.
- [50] Paweł Wiczling, Roman Kaliszan, “Retention time and peak width in the combined pH/organic modifier gradient high performance liquid chromatography”, *Journal of Chromatography A*, 1217 (2010) 3375 – 3381.
- [51] Carlo Bicchi, Chiara Cordero, Cristina Iori, Patrizia Rubiolo, “Headspace sorptive extraction (HSSE) in the headspace analysis of aromatic and medicinal plants”, *J. High Resol. Chromatography*, 23 (2000) 539 – 546.
- [52] V. M. León, B. Álvarez, M. A. Cobollo, S. Muñoz, I. Valor, “Analysis of 35 priority semivolatile compounds in water by stir bar sorptive extraction-thermal desorption-gas chromatography-mass spectrometry”, *Journal of Chromatography A*, 999 (2003) 91 – 101.
- [53] Erik Baltussen, Frank David, Pat Sandra, Hans-Gerd Janssen, Carel A. Cramers, “Equilibrium sorptive enrichment on poly(dimethylsiloxane) particles for trace analysis of volatile compounds in gaseous samples”, *Anal. Chem.*, 71 (1999) 5193 – 5198.
- [54] Ben V. Burger, Brenda Marx, Maritha le Roux, Wina J. G. Burger, “Simplified analysis of organic compounds in headspace and aqueous samples by high-capacity sample enrichment probe”, *Journal of Chromatography A*, 1121 (2006) 259 – 267.
- [55] <http://www.polyurethanes.org/index.php?page=what-is-it> (Agosto de 2012).
- [56] M. Graymore, F. Stagnitti, G. Allison, “Impacts of atrazine in aquatic ecosystems”, *Environment International*, 26 (2001) 483 – 495.
- [57] Simón Navarro, Nuria Vela, M^a José Giménez, Ginés Navarro, “Effect of temperature on the disappearance of four triazine herbicides in environmental waters”, *Chemosphere*, 57 (2004) 51 – 59.
- [58] Jae Jak Nam and Sang Hak Lee, “GC-MS/MS Analysis of benzo(a)pyrene by ion trap tandem mass spectrometry”, *Korean Chem. Soc.*, 2002, Vol. 23, No 8.
- [59] <http://www.sigmaaldrich.com/portugal.html> (Agosto de 2012)

[60] http://en.wikipedia.org/wiki/List_of_R-phrases (Agosto de 2012)

[61] http://en.wikipedia.org/wiki/List_of_S-phrases (Agosto de 2012)

Appendixes

Appendix I

I.1 Chromatogram

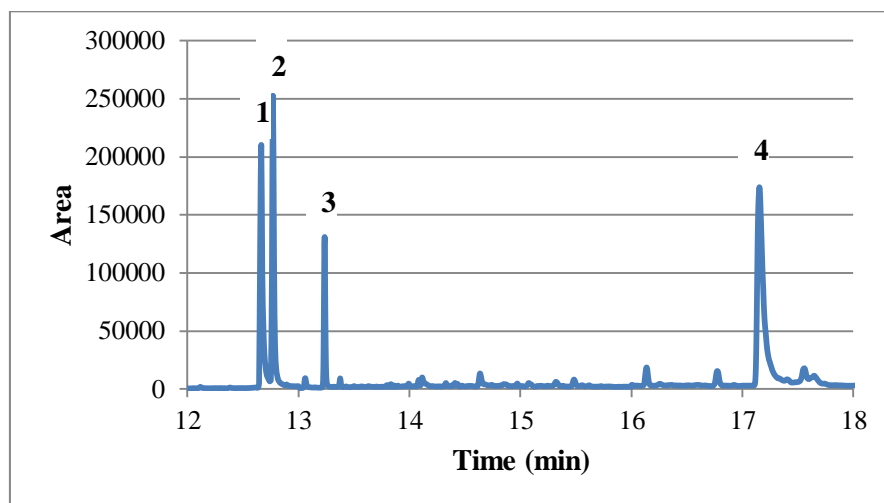


Figure I.1.1 - Chromatogram of the control sample. **1** – ATZ, **2** – TBZ, **3** – ALA, **4** – B(a)P.

Appendix II

II.1 Linearity plots

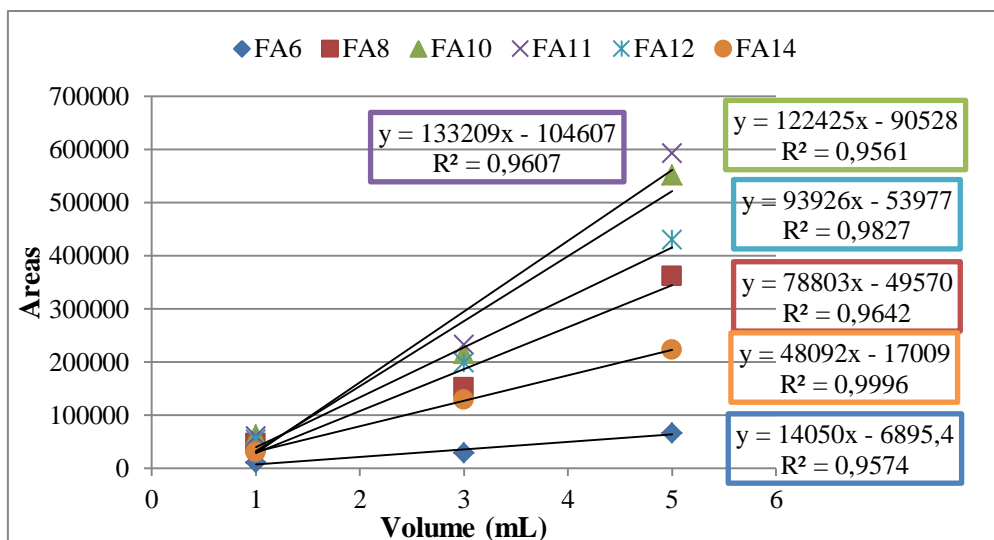


Figure II.1. 1 – Linearity plots of the influence of volume sample (with 0.20 mL/min of flow rate of sample, 0.10 mL/min of flow rate of EtAc and 30 minutes of drying at 1 bar).

II.2 Calibration plots

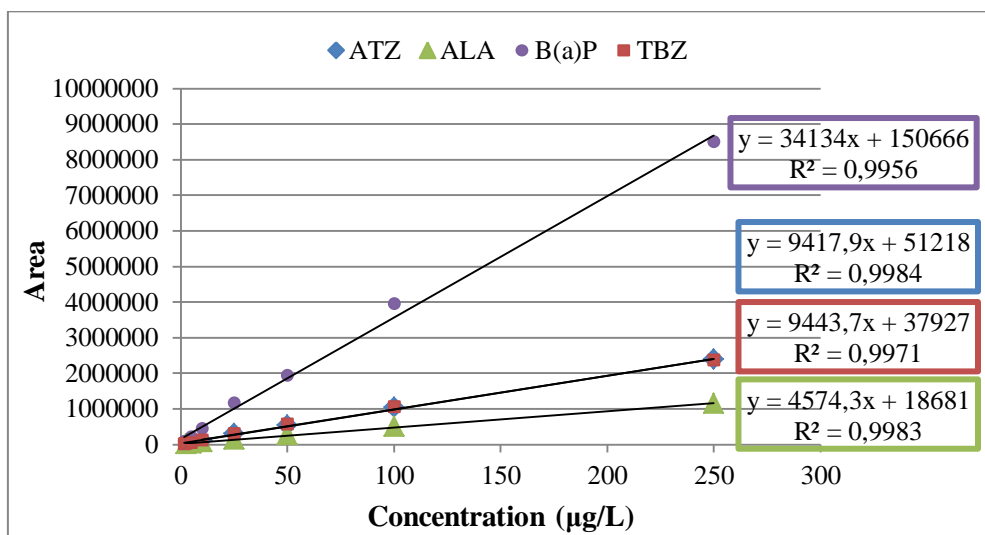


Figure II.2.1 – Instrumental calibration of the compounds under optimized GC-MS(SIM) conditions.

II.3 Regression plots

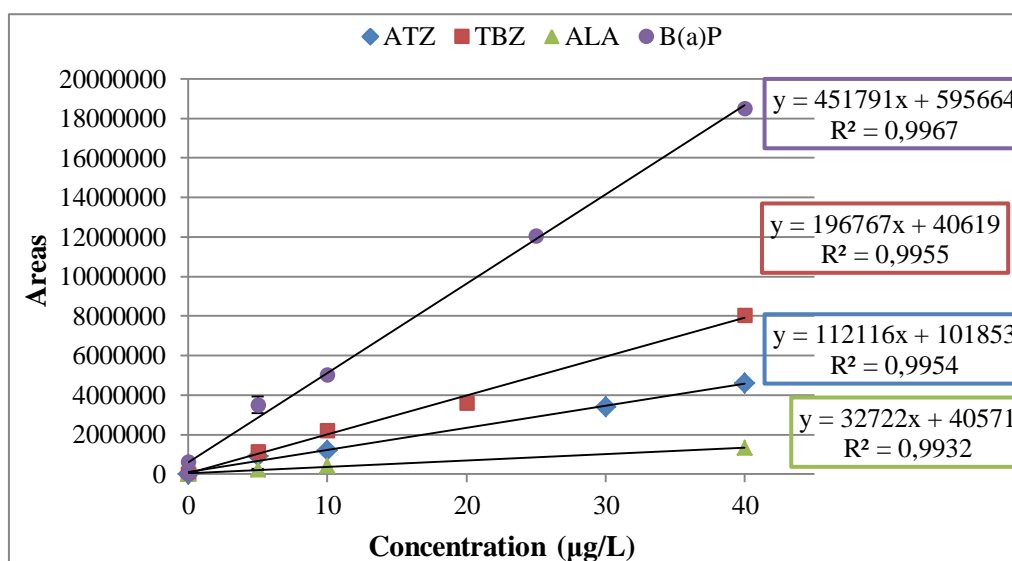


Figure II.3.1 – Regression plots of the compounds obtained from SAM, under optimized conditions, for the surface water sample.

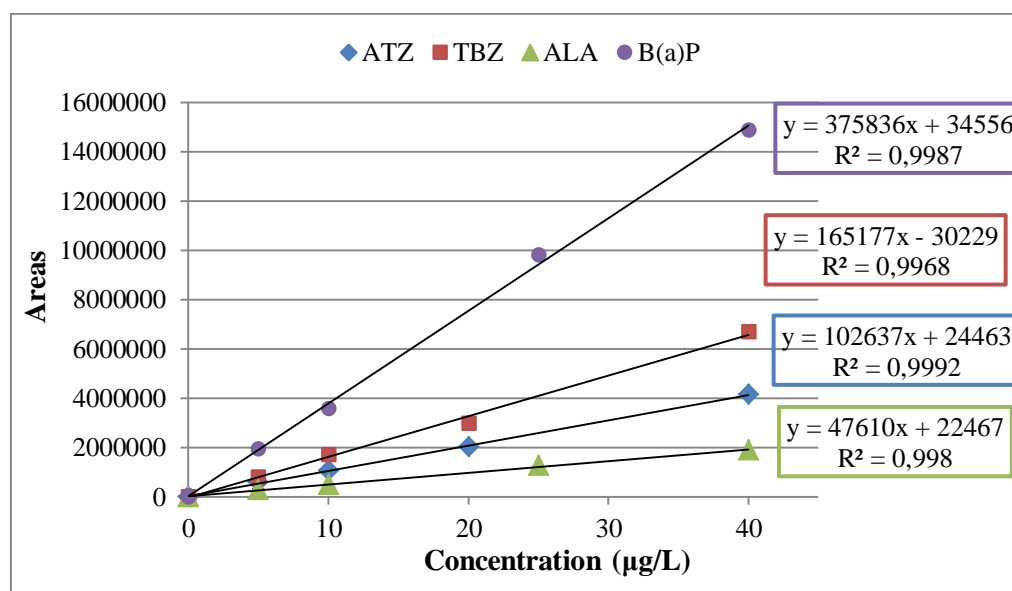


Figure II.3.2 – Regression plots of the compounds obtained from SAM, under optimized conditions, for the ground water sample.

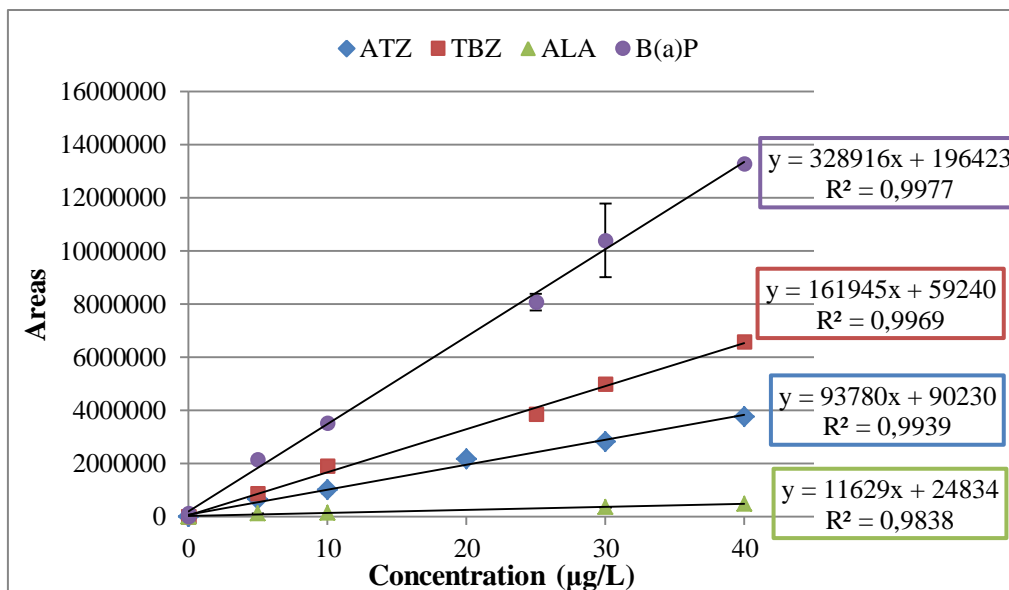


Figure II.3.3 – Regression plots of the compounds obtained from SAM, under optimized conditions, for the tap water sample.

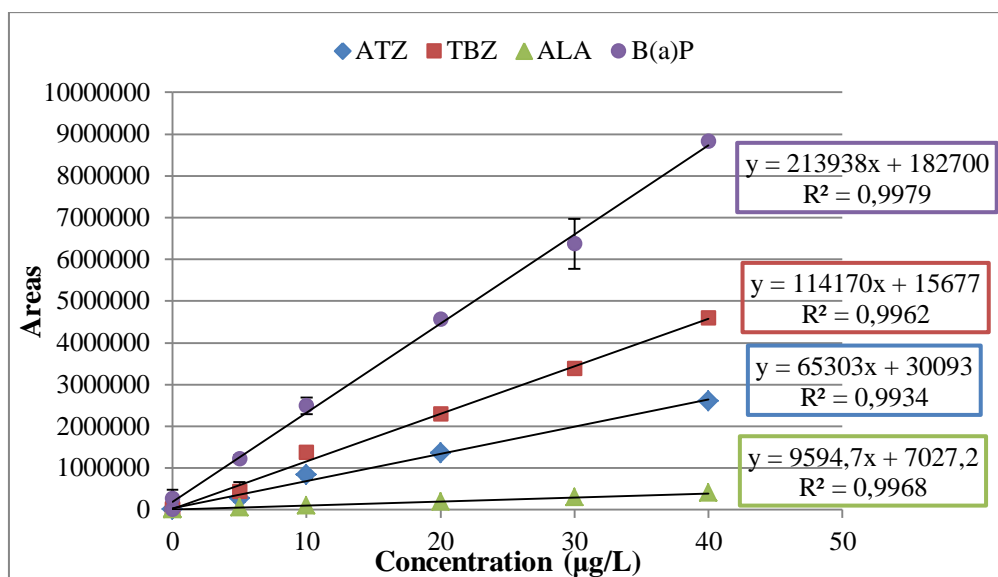


Figure II.3.4 – Regression plots of the compounds obtained from SAM, under optimized conditions, for the seawater sample.

Appendix III

III.1 Speciation of the analytes as a function of the pH, obtained by the SPARCS program

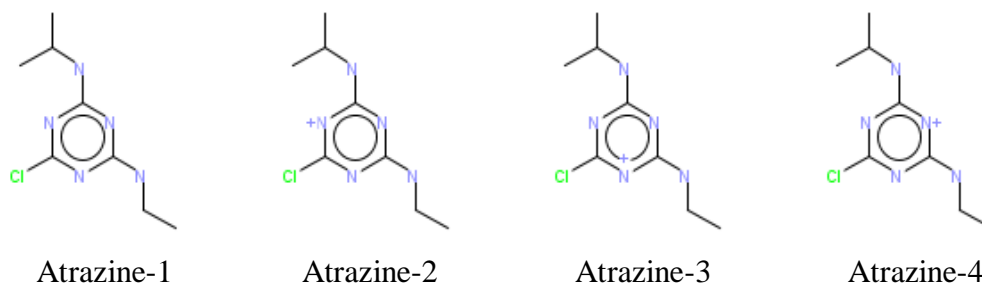


Figure III.3.1 – Possible ionization forms for atrazine obtained by the SPARCS program.

Table III.3.1 – Proportion of the neutral and the ionize species of atrazine in function of the pH.

pH	Atrazine-1	Atrazine-2	Atrazine-3	Atrazine-4
0.2	0.08	0.12	0.11	0.69
1	0.37	0.08	0.08	0.48
2	0.85	0.02	0.02	0.11
3	0.99	0	0	0.01
4	1	0	0	0
5	1	0	0	0
6	1	0	0	0
7	1	0	0	0
8	1	0	0	0
9	1	0	0	0
10	1	0	0	0
11	1	0	0	0
12	1	0	0	0
13	1	0	0	0
14	1	0	0	0

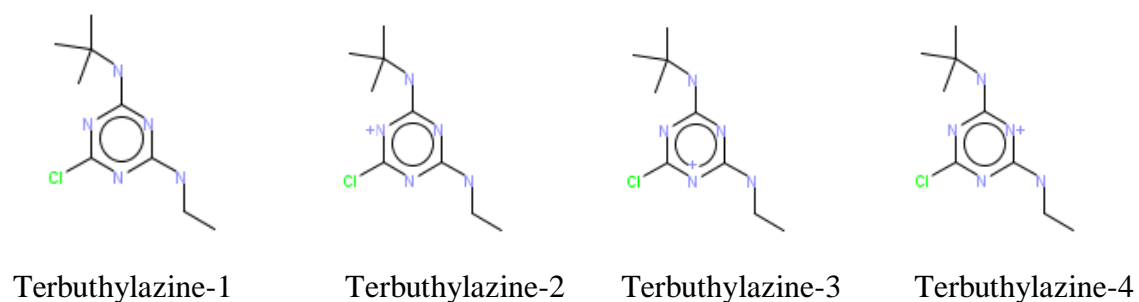
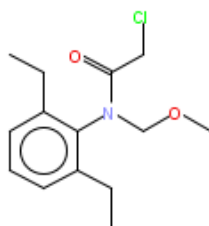


Figure III.3.2 – Possible ionization forms for terbutylazine obtained by the SPARCS program.

Table III.3.2 – Proportion of the neutral and the ionize species of terbutylazine in function of the pH.

	Terbutylazine-1	Terbutylazine-2	Terbutylazine-3	Terbutylazine-4
pH	1	2	3	4
0.2	0.10	0.12	0.10	0.69
1	0.40	0.08	0.06	0.45
2	0.87	0.02	0.01	0.10
3	0.99	0	0	0.01
4	1	0	0	0
5	1	0	0	0
6	1	0	0	0
7	1	0	0	0
8	1	0	0	0
9	1	0	0	0
10	1	0	0	0
11	1	0	0	0
12	1	0	0	0
13	1	0	0	0
14	1	0	0	0



Alachlor-1

Figure III.3.3 – Possible ionization form for alachlor obtained by the SPARCS program.

Table III.3.3 – Proportion of the species of alachlor in function of the pH.

pH	Alachlor-1
0.2	1
1	1
2	1
3	1
4	1
5	1
6	1
7	1
8	1
9	1
10	1
11	1
12	1
13	1
14	1



Benzo(a)pyrene-1

Figure III.3.4 – Possible ionization form for benzo(a)pyrene obtained by the SPARCS program.

Table III.3.4 – Proportion of the species of benzo(a)pyrene in function of the pH.

pH	Benzo(a)pyrene-1
0.2	1
1	1
2	1
3	1
4	1
5	1
6	1
7	1
8	1
9	1
10	1
11	1
12	1
13	1
14	1

Appendix IV

IV.1 Formulas

The calculation of the mean (\bar{X}), standard deviation (σ) and the application of the least squares method (linearization) were performed by using pre-defined functions of the Microsoft excel.

The relative standard deviation (RSD) was determinate using the following formula,

$$RSD (\%) = \left(\frac{\sigma}{\bar{X}} \right) \times 100$$

The recovery was calculated using the expression,

$$Recovery (\%) = \left(\frac{A_{obt}}{A_{exp}} \right) \times 100$$

Were, A_{obt} is the obtained Area and A_{exp} is the expected Area.

On the other hand, the desorption efficiency (E) was considered through the following relation,

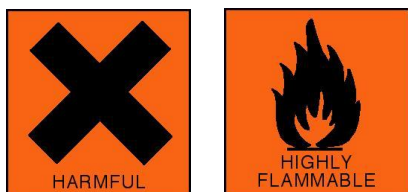
$$E (\%) = \left(\frac{A_f}{A_T} \right) \times 100$$

Were, A_f is the Area of the Fraction and A_T is the Total Area (sum of the areas of the first and second fraction).

Appendix V

V.1 MSDS files of the solvents

- Ethyl Acetate ($\text{C}_4\text{H}_8\text{O}_2$)



R: 11, 36, 66, 67.

S: 16, 26, 33.

Boiling point: 76.5 °C.

- Methanol (CH_3OH)



R: 11, 23, 24, 25, 39.

S: 7, 16, 36, 37, 45.

Boiling point: 64.7 °C.

- Dichloromethane (CH_2Cl_2)



R: 20, 22, 40.

S: 23, 24, 25, 36, 37.

Boiling point: 40 °C.

- Acetonitrile (CH_3CN)



R: 11, 20, 21, 22, 36.

S: 16, 36, 37.

Boiling point: 81 °C.

- n-Hexane (C_6H_{14})



R: 11, 20, 38, 48, 51, 53, 62, 65, 67.

S: 16, 36, 37, 39, 45, 53.

Boiling point: 69 °C.

- Hydrochloric Acid (HCl)



R: 23, 24, 25, 34, 36, 37, 38.

S: 26, 36, 37, 39, 45.

Boiling point: 109 °C.

V.2 MSDS files of the reagents

- Sodium Hydroxide (NaOH)



R: 35.

S: 26, 37, 39, 45.

- Atrazine ($\text{C}_8\text{H}_{14}\text{ClN}_5$)



R: 22, 43, 48, 50, 53.

S: 16, 36, 37.

- Terbutylazine ($\text{C}_9\text{H}_{16}\text{ClN}_5$)



R: 22.

S: 36.

- Alachlor ($\text{C}_8\text{H}_{14}\text{ClN}_5$)



R: 22, 40, 43, 50, 53.

S: 36, 37, 46, 60, 61.

- Toluene (C_7H_8)



R: 11, 20, 38, 48, 63, 65, 67.

S: 36, 37, 46, 62.

- Ethylbenzene (C_8H_{10})



R: 11, 20.

S: 16, 24, 25, 29.

- p-Xylene (C_8H_{10})



R: 10, 20, 21, 38.

S: 25.

- Methyl Octanoate ($C_9H_{18}O_2$)



R: 38.

- Methyl Undecanoate ($C_{12}H_{24}O_2$)



R: 41.

S: 39.

- Methyl Myristate ($C_{15}H_{30}O_2$)



R: 38.

- Methyl Decanoate ($C_{11}H_{22}O_2$)



R: 38.

- Fluoranthene ($C_{16}H_{10}$)



R: 22, 50.

S: 61.

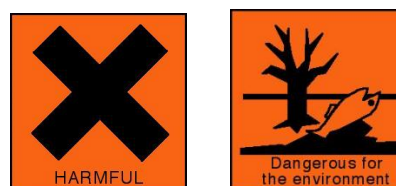
- Anthracene ($C_{14}H_{10}$)



R: 36, 37, 38, 50, 53.

S: 26, 60, 61.

- Phenanthrene ($C_{14}H_{10}$)



R: 22, 36, 37, 38, 50.

S: 26, 60, 61.

- Naphtalene ($C_{10}H_8$)



R: 22, 40, 50, 53.

S: 36, 37, 46, 60, 61.

- Pyrene ($C_{16}H_{10}$)



R: 50, 53.

S: 60, 61.

V.3 List of R-phrases

R10: Flammable.

R11: Highly flammable.

R20: Harmful by inhalation.

R21: Harmful in contact with skin.

R22: Harmful if swallowed.

R23: Toxic by inhalation.

R24: Toxic in contact with skin.

R25: Toxic if swallowed.

R34: Causes burns.

R35: Causes severe burns.

R36: Irritating to eyes.

R37: Irritating to respiratory system.

R38: Irritating to skin.

R39: Danger of very serious irreversible effects.

R40: Limited evidence of carcinogenic effect.

R41: Risk of serious damage to eyes.

R43: May cause sensitization by skin contact.

R48: Danger of serious damage to health by prolonged exposure.

R50: Very toxic to aquatic organisms.

R51: Toxic to aquatic organisms.

R53: May cause long-term adverse effects in the aquatic environment.

R62: Possible risk of impaired fertility.

R63: Possible risk of harm to the unborn child.

R65: Harmful: may cause lung damage if swallowed.

R66: Repeated exposure may cause skin dryness or cracking.

R67: Vapours may cause drowsiness and dizziness.

V.4 List of S-phrases

S7: Keep container tightly closed.

S16: Keep away from sources of ignition – No smoking.

S23: Do not breathe gas/ fumes/ vapour/ spray (appropriate wording to be specified by manufacturer).

S24: Avoid contact with skin.

S25: Avoid contact with eyes.

S26: In case of contact with eyes, rinse immediately with plenty of water and seek medical advice.

S29: Do not empty into drains.

S33: Take precautionary measures against static discharges.

S36: Wear suitable protective clothing.

S37: Wear suitable gloves.

S39: Wear eye/ face protection.

S45: In case of accident or if you feel unwell seek medical advice immediately (show the label where possible).

S46: I swallowed, seek medical advice immediately and show this container or label.

S53: Avoid exposure – obtain special instructions before use.

S60: This material and its container must be disposed of as hazardous waste.

S61: Avoid release to the environment. Refer to special instructions/ safety data sheet.

S62: If swallowed, do not induce vomiting: seek medical advice immediately and show this container or label where possible.